Self-assembled prebiotic amphiphile-mixture exhibit tunable catalytic properties

Raki Mandal, Anupam Ghosh, Nilesh K. Rout, Mahesh Prasad, Bibhas Hazra, Sanu Sar, Subrata Das, Ayan Datta, and Pradip K. Tarafdar*

*Corresponding author: Dr. Pradip Kumar Tarafdar

Email: tarafdar@iiserkol.ac.in, srpradip@gmail.com

Table of Contents

Title	Page
General information	S2
Dry-down reaction and synthesis of OLH, NLH, OLS, NLS	S2
Measurement of critical Micellar concentration (CMC)	S8
Standard curve of *p*-nitrophenol at 400nm, at 347 nm, and esterase activity	S9
Surface charge (CTAB, SDBS) tunes the catalytic efficiency of OLH	S15
Role of acyl chain length of catalysts	S16
Substrate selectivity of the catalyst OLH	S17
Methylation of histidine amine, pK_a perturbation, and substrate selectivity	S17
Mechanistic studies of hydrolysis	S19
Kinetics parameter determination of OLH, OLDMH, OLTMH	S21
Zeta potential measurement	S22
The synthetic procedure of amphiphiles and NMR spectra	S22
References	S43

General Information: Reactions were performed under an inert (N_2) atmosphere using pre-dried glassware and standard reaction flasks. Substrates obtained from commercial sources (Alfa Aesar, Sigma-Aldrich, Avra Synthesis Private Limited, Sisco Research Laboratories) were used without further purification. Yields refer to isolated compounds. Thin layer chromatography (TLC) was performed on Merck precoated silica gel 60 F254 aluminum sheets with detection under UV light at 254 nm. Chromatographic separations were carried out on Chempure silica gel (60-120 mesh or 100-200 mesh). High-resolution mass spectra (HRMS, m/z) were recorded on Bruker Micro-TOF and Water HRMS spectrometry. Zeta potential was measured on Malvern Zetasizer Nano ZS, UK. UV measurements were performed on BioTek, Epoch Microplate Reader, and Fluorescence spectra were measured with F-7000, HITACHI spectrofluorometer. Nuclear magnetic resonance (NMR) spectroscopy was performed using JEOL 400 MHz and Bruker 500 MHz spectrometers. Chemical shifts (δ) are provided in ppm. IUPAC names were obtained from ChemDraw software. Milli-Q water was used in all the experiments.

Dry-down reactions:

Prebiotic synthetic route of O-lauroyl histidine (OLH):

We performed a dry-down reaction with L-histidine and lauryl alcohol (1:1 mixture, 40 mM each) in pH 3.0 buffer at 90 ^{o}C under atmospheric pressure. After two wet-dry cycles at 90 ^{o}C over a period of 24 hours, we checked the mass spectrum of the reaction mixture. We observed the corresponding ester (OLH) peak at m/z = 324.2655 (expected m/z = 324.2651). This observation indicated that a dry-down reaction might be a plausible pathway for the synthesis of amino acid esters during early evolution from a mixture of amino acid and alcohol. We synthesized OLH by general protection and deprotection method **(see the synthetic procedure of OLH),** and we found the mass of the synthesized compound is 324.2648 (**Figure S1**).

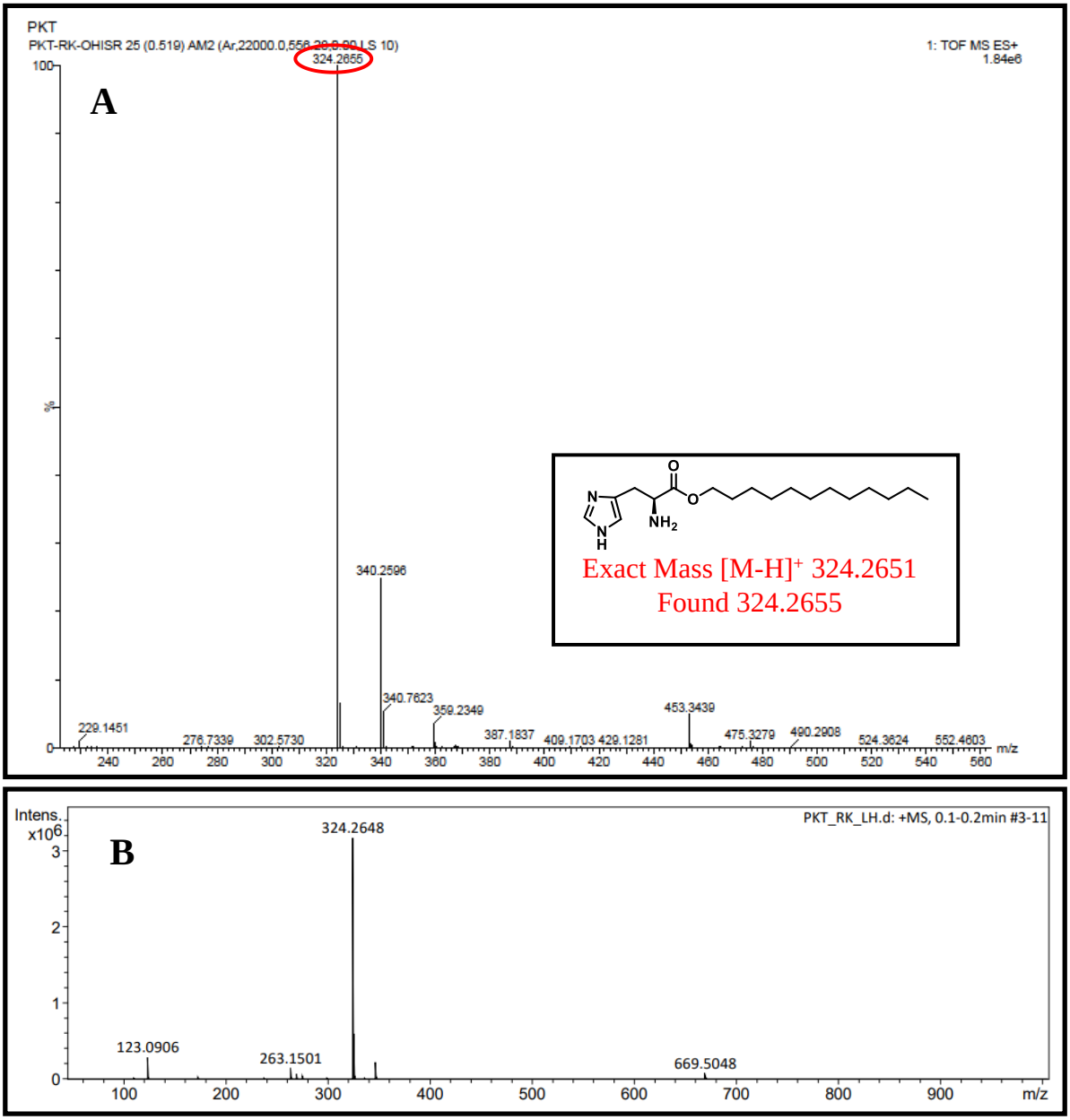

Figure S1: Detection of OLH by HRMS. A) Detection of OLH from dry-down reactions with histidine and lauryl alcohol. B) Mass spectrum of the synthesized OLH.

The ^{1}H-NMR of the crude reaction mixture was recorded and compared with the ^{1}H-NMR of the synthesized compound (OLH). We found the presence of new peaks at 7.81 ppm, 7.02 ppm, 4.23 ppm, 4.08 ppm, 3.05 ppm, 1.50 ppm, 0.80 ppm (a to g protons), which likely corresponds to *O*-lauryl histidine (OLH) (**Figure S2**). The mild shift of chemical shift(s) of the aromatic protons and the protons near the aromatic ring is due to the protonation-deprotonation of imidazole and ammonium groups.

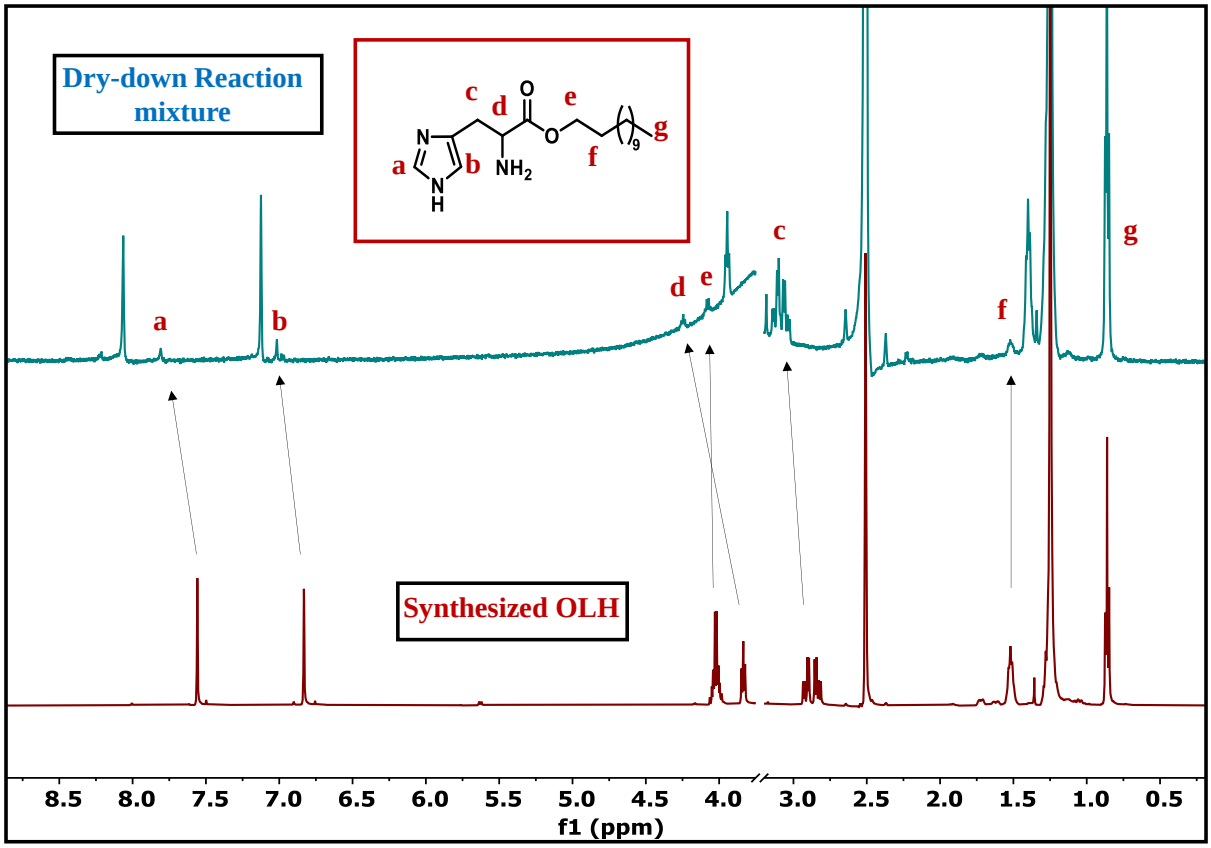

Figure S2: Stacking plot of ^{1}H-NMR Synthesized compound OLH and dry down reaction mixture (histidine, lauryl alcohol, and OLH).

Prebiotic synthetic route of N-lauroyl histidine (NLH):

We performed a dry-down reaction with L-histidine and lauric acid (1:1 mixture, 40 mM each) in pH 3.0 buffer at 90 ^{o}C under atmospheric pressure. After two wet-dry cycles at 90 ^{o}C over a period of 24 hours, we checked the mass spectrum of the reaction mixture. We observed the corresponding amide (NLH) peak at m/z $[M-H]^{+}$ = 338.2451 (expected m/z = 338.2444). This observation indicated that dry-down reaction might be a plausible pathway for the synthesis of amino acid amide during early evolution from a mixture of amino acid and carboxylic acid. We synthesized NLH by standard method **(see the synthetic procedure of NLH),** and we found the mass of the synthesized compound is $[M-H]^{+}$ = 338.2424 (**Figure S3**).

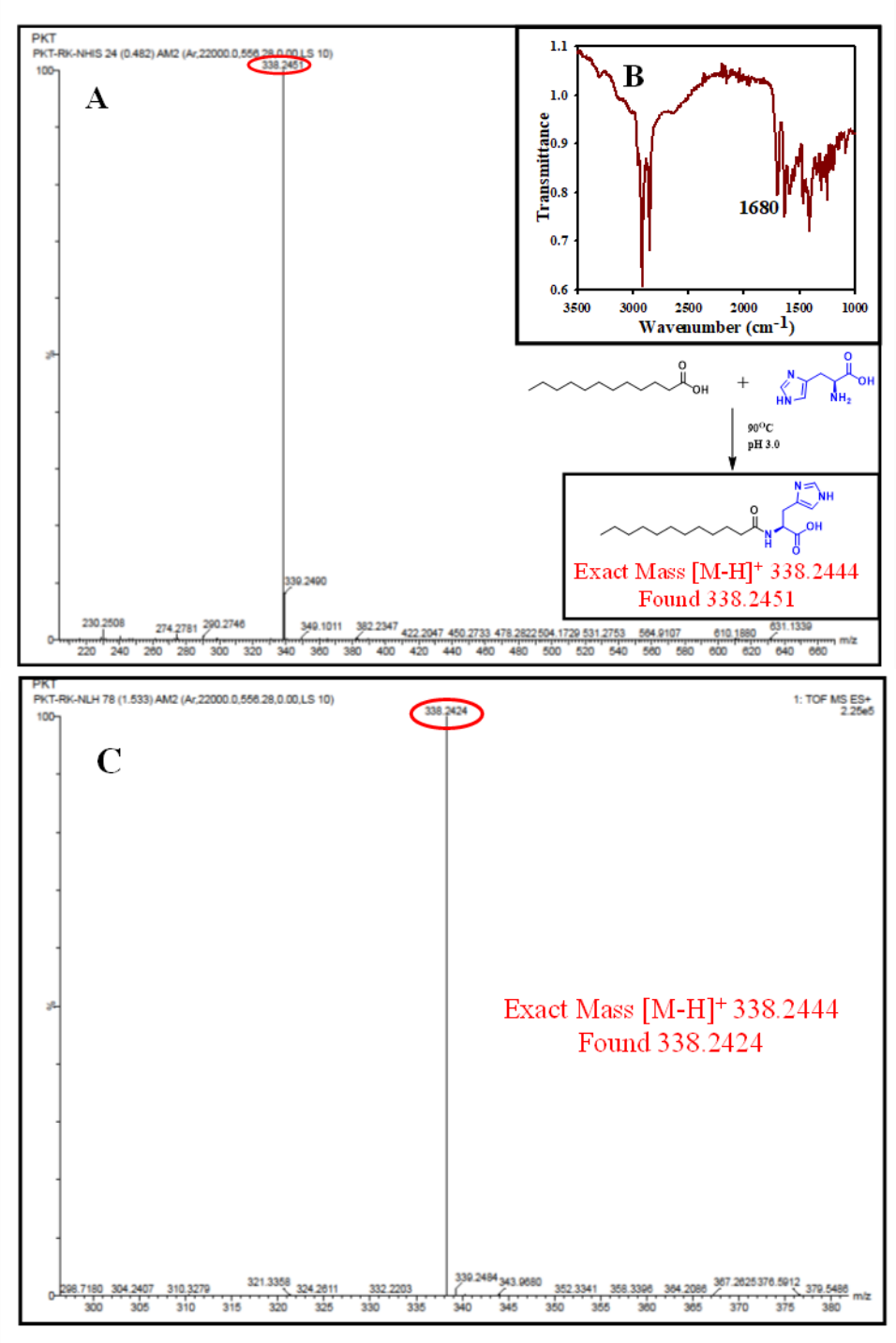

Figure S3: Detection of NLH by HRMS and IR spectra. A) Detection of NLH by HRMS from dry-down reactions with L-histidine and lauric acid. B) IR spectra of the dry-down reaction mixture of L-histidine and lauric acid. C) Mass spectra of synthesized NLH.

Prebiotic synthetic route of O-lauroyl serine (OLS):

We performed dry-down reaction with L-Serine and lauryl alcohol (1:1 mixture, 40 mM each) in pH 3.0 buffer at 90 ºC. After two wet-dry cycles over a period of 24 hours, we checked the

mass spectrum of the reaction mixture. We observed the corresponding ester (OLS) peak at m/z = 274.2797 (expected m/z = 274.2382). This observation indicated that dry-down reaction might be a plausible pathway for the synthesis of amino acid esters during early evolution from a mixture of amino acid and alcohol. We synthesized OLS by general protection and deprotection method **(see the synthetic procedure of OLS)** and we found the mass of the synthesized compound is 274.2378. The presence of 1735 cm^{-1} peak suggests the presence of an ester bond (**Figure S4**).

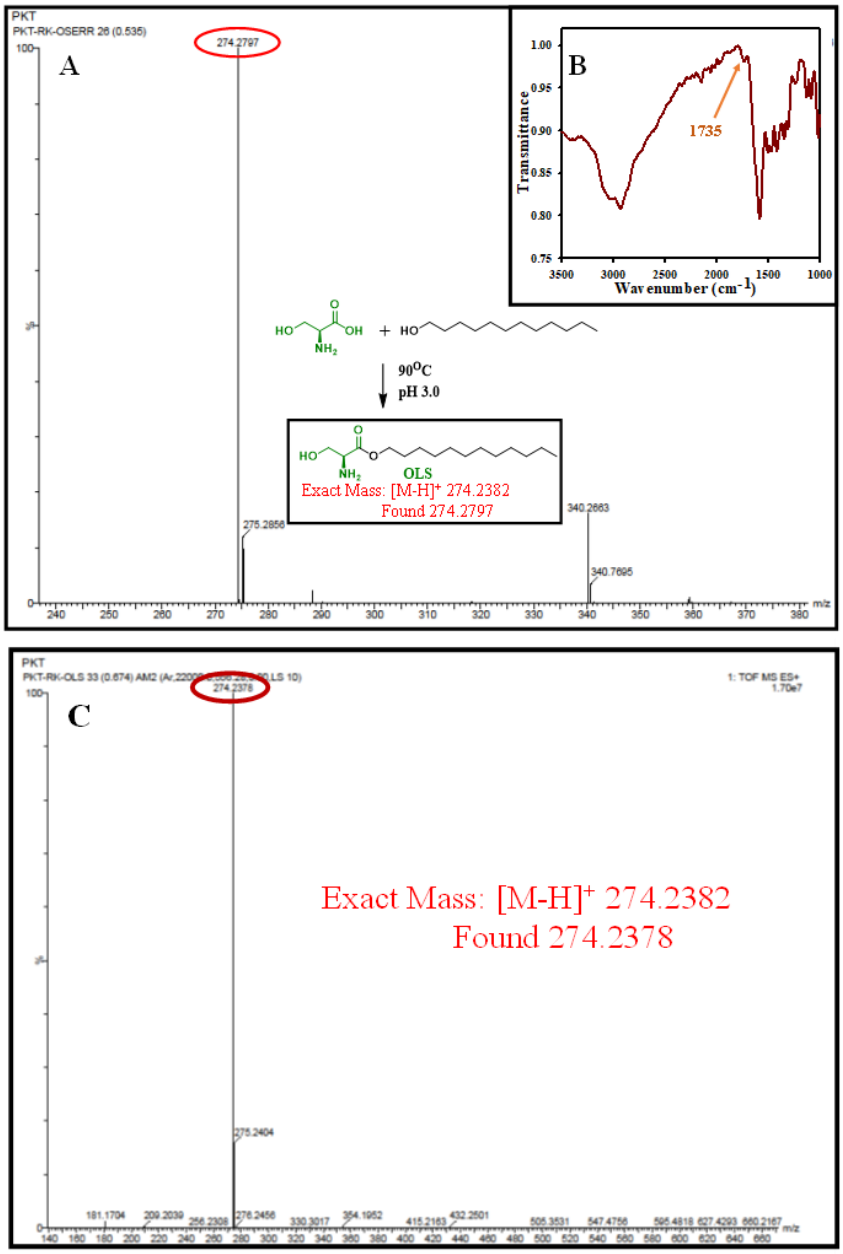

Figure S4: Detection of OLS by mass and IR spectra. A) Detection of OLS by mass from dry-down reactions with L-serine and lauryl alcohol. B) IR spectra of the dry-down reaction mixture of serine and lauryl alcohol. C) Mass spectra of synthesized OLS.

Prebiotic synthetic route of N-lauroyl serine (NLS):

We performed dry-down reaction with L-serine and lauric acid (1:1 mixture, 40 mM each) in pH 3.0 buffer at 90 ^{o}C under atmospheric pressure. After two wet-dry cycles at 90 ^{o}C over a period of 24 hours, we checked the mass spectrum of the reaction mixture. We observed the corresponding ester (NLS) peak at m/z $[M\text{-}Na]^{+}$ = 310.1965 (expected m/z = 310.1994). We synthesized NLS by general protection and deprotection method **(see the synthetic procedure of NLS),** and we found the mass of the synthesized compound is $[M\text{-}H]^{+}$ = 288.2164. The presence of 1677 cm^{-1} suggests the presence of an amide bond (**Figure S5**).

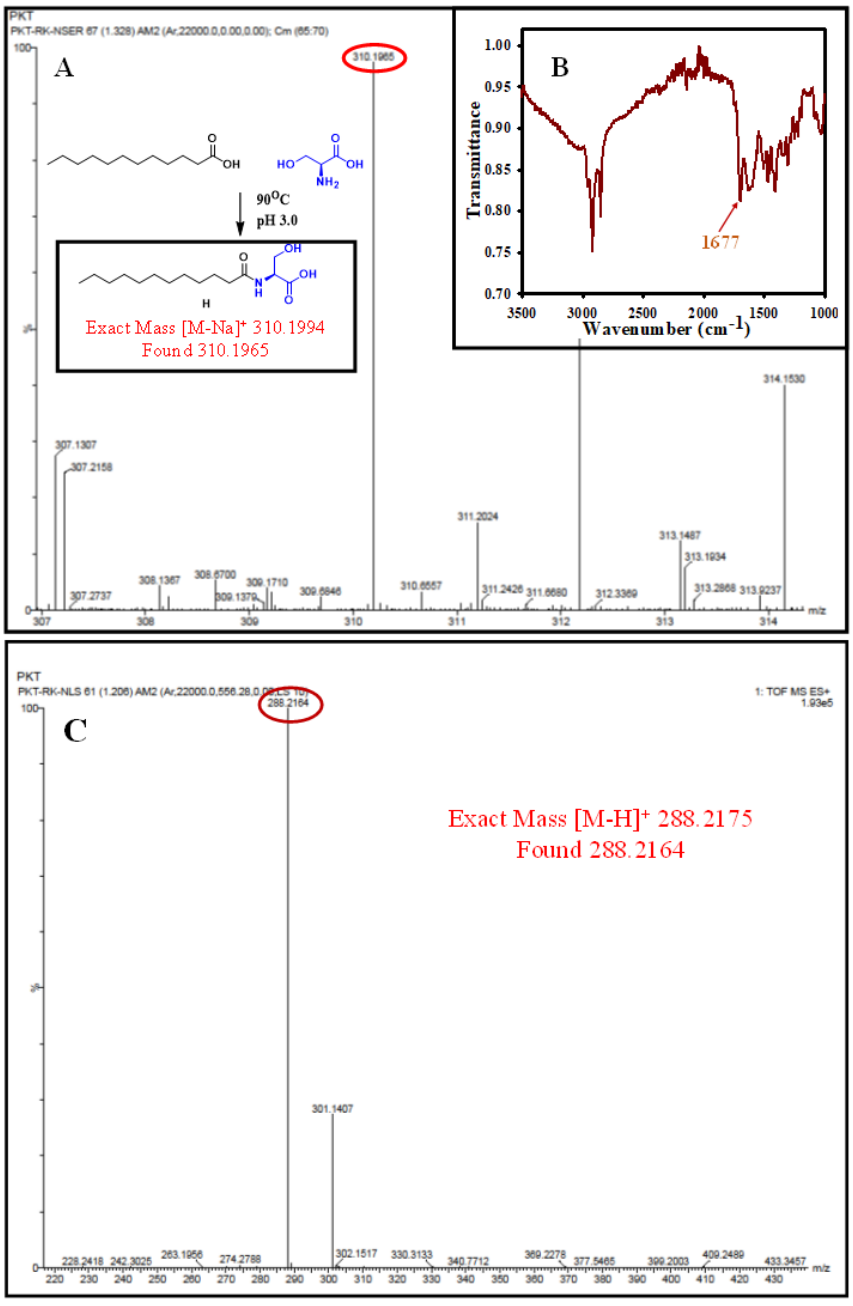

Figure S5: Detection of NLS by HRMS and IR spectra. A) Detection of NLS by HRMS from dry-down reactions with L-serine and lauric acid. B) IR spectra of the dry-down reaction mixture of L-serine and lauric acid. C) Mass spectra of synthesized NLS.

Critical micellar concentration (CMC) determination using pyrene fluorescence: CMC was measured using pyrene by fluorometric analysis. Initially, pyrene was in a buffer (hydrophilic environment), and its concentration was 1 µM. Samples were excited at 334 nm, and emission spectra were recorded in the range between 350 and 550 nm. The excitation and emission slit widths were set at 2.5 nm. I_1/I_3 (intensity ratio of first and third peak, pyrene has five fluorescence bands) value remains high (around 1.8) when it is in the hydrophilic region (aqueous medium). We gradually added the amphiphile to this solution and recorded the spectra. When pyrene resides in the hydrophobic region (after self-assembly) the I_1/I_3 value became lower. The I_1/I_3 ratio was plotted at various concentrations of lipidated amino acids (amphiphiles), and the data were fitted to the sigmoidal equation. From the fit, the CMC was determined. The CMC value of OLH is approximately 0.078 mM. CMC of *O*-octyl histidine (OOH) was ~ 30-fold higher than *O*-lauryl histidine (2.58 mM) because of the presence of shorter lipid chains. The CMC value of OLS is approximately 0.077 mM. CMC of OLDMH, OLTMH, and NLH are 0.05 mM, 0.1 mM, and 0.05 mM, respectively.

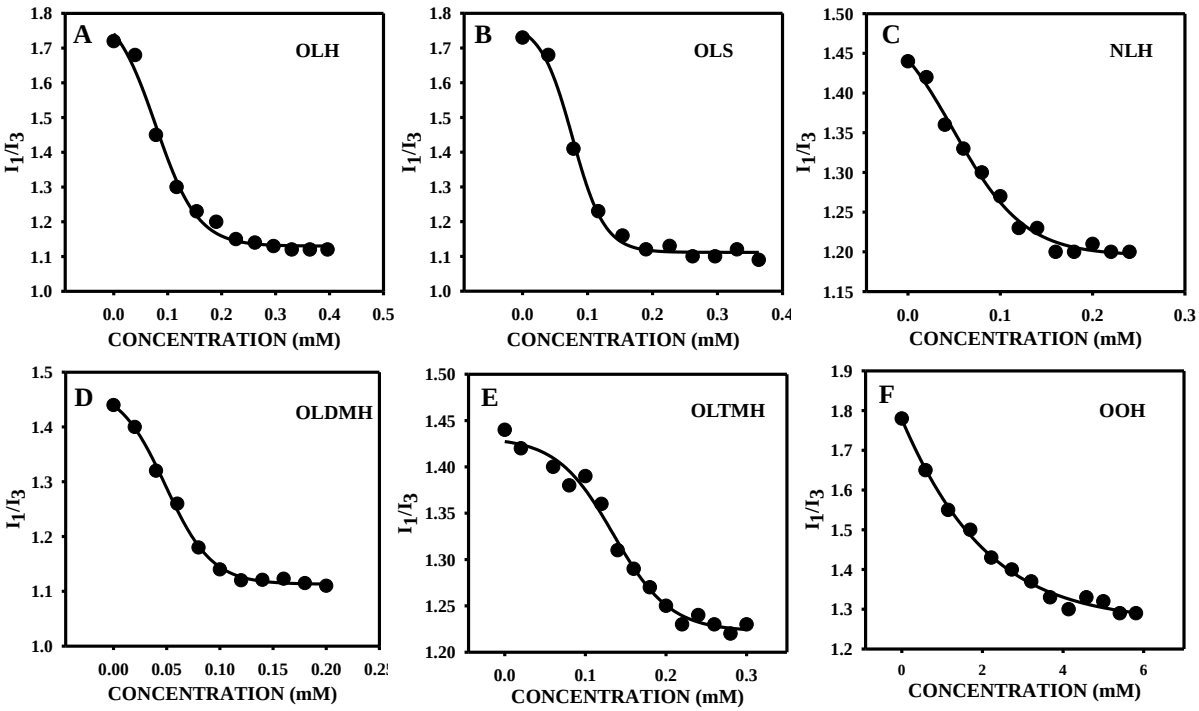

Figure S6: CMC determination of amphiphiles.

Standard curve of *p*-nitro phenol at 400 nm: Butyl *p*-nitrophenol (BP) (the synthetic procedure given below) was used as the substrate compound to check the esterase activity of amphiphiles. The postulate was if the catalyst broke the ester bond, the liberated *p*-nitrophenol could be monitored by UV-Vis spectrophotometer. A standard curve for *p*-nitrophenol was plotted to keep track of how much *p*-nitrophenol was formed to calculate the % hydrolysis.

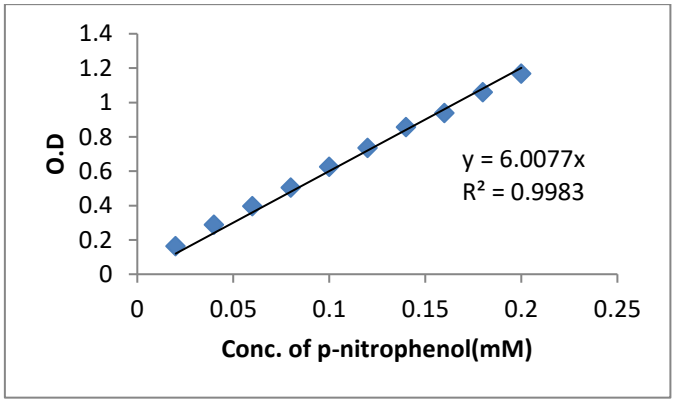

Figure S7: Standard curve of *p*-nitrophenol at pH 7.0. Optical density (OD) was measured at 400 nm.

Esterase activity: The reaction progress was followed spectrophotometrically by monitoring the liberation of *p*-nitrophenol at λmax = 400 nm as a function of time. 0.5 mM butyl- *p*-nitro phenol (BP) was used as substrate at pH 7.0 in 20 mM tris buffer. Lipidated amino acids were added to the buffer (the final concentration of each amphiphile was 0.1 mM) and the absorbance was recorded in a Biotek microplate reader. In all cases, the background hydrolysis was subtracted. The % of hydrolysis was calculated by using the molar extinction coefficient value of *p*-nitro phenol, 6007 $M^{-1}cm^{-1}$, and plotted with time. The initial rate (a*b) was calculated by fitting the kinetic data (concentration of product vs time) into the mono-exponential equation ($y = a(1 - e^{-bx}$).

Standard curve of *p*-nitro phenol (at 347nm): Butyl *p*-nitrophenol (BP) (the synthetic procedure given below) was used as the substrate compound to check the esterase activity of amphiphiles. The postulate was if the catalyst broke the ester bond, the liberated *p*-nitrophenol could be monitored by UV-Vis spectrophotometer. A standard curve for *p*-nitrophenol (at isobestic point) was plotted to keep track of how much *p*-nitrophenol was formed to calculate the % hydrolysis.

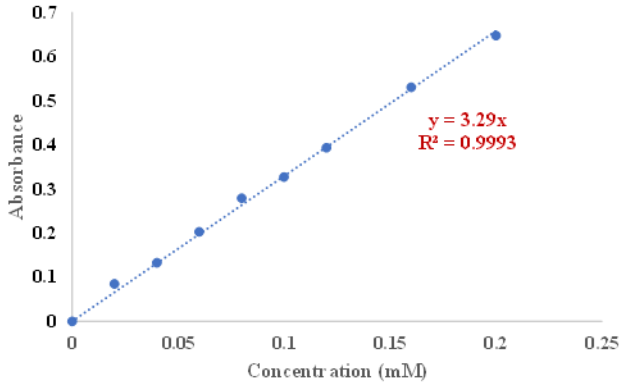

Figure S8: Standard curve of *p*-nitrophenol at pH 7.0 at 347 nm.

The surface may modulate the pK_a of *p*-nitrophenol/*p*-nitrophenolate equilibrium.[1] So, there is a possibility to change the absorbance value of *p*-nitophenolate at 400nm at different ionic surfaces. The spectra of *p*-nitrophenol in the presence of various surfaces at pH 7.0 buffer were recorded. We found that the absorbance (at 400nm) of 0.08 mM *p*-nitrophenol is nearly same at various surfaces. The absorbance at 320nm of 0.08 mM *p*-nitrophenol is also nearly the same at various surfaces. We can monitor the kinetics at 400 nm or at the isosbestic point (at 347nm).

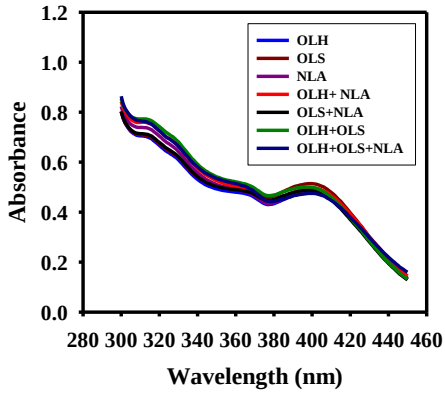

Figure S9: A) Wavelength scan of 0.08 mM *p*-nitrophenol at various surface. The pH was 7.0.

Esterase activity at 347 nm: The reaction progress was followed spectrophotometrically by monitoring the liberation of *p*-nitrophenol at 347 nm as a function of time. 0.5 mM butyl- *p*-nitro phenol (BP) was used as substrate at pH 7.0 in 20 mM tris buffer. Lipidated amino acids were added to the buffer (the final concentration of each amphiphile was 0.1 mM) and the absorbance was recorded in a Biotek microplate reader. In all cases, the background hydrolysis was subtracted. The % of hydrolysis was calculated by using the molar extinction coefficient value of *p*-nitro phenol at 347 nm, 3290 $M^{-1}cm^{-1}$, and plotted with time.

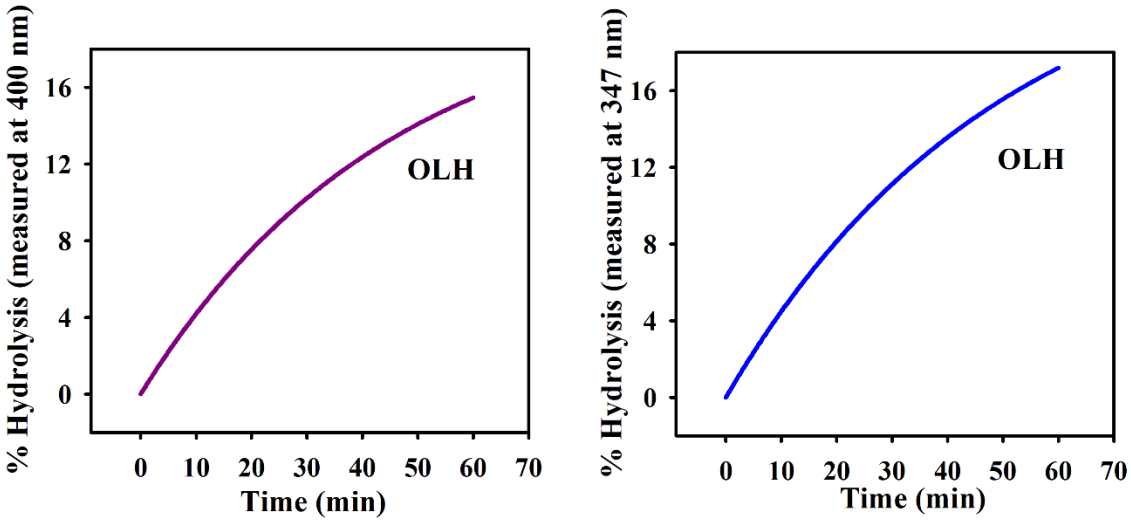

Figure S10: Hydrolytic activity of 0.1 mM OLH. **Left panel:** Release of *p*-nitrophenol monitored at 400 nm, **right panel:** Release of *p*-nitrophenol monitored at 347 nm. The comparable extent of hydrolysis suggest that further experiments can be performed at 400 nm.

Esterase activity in the presence of 12.5% DMSO: The reaction progress was followed spectrophotometrically by monitoring the liberation of *p*-nitrophenol at λmax = 400 nm as a function of time. 0.5 mM butyl- *p*-nitro phenol (BP) was dissolved at pH 7.0 (20 mM tris buffer) with 12.5 % DMSO. Then 0.1 mM OLH was added to the DMSO dopped buffer, and the absorbance was recorded in a Biotek microplate reader. In the presence of DMSO (12.5%), no hydrolysis was observed (**Figure S11**).

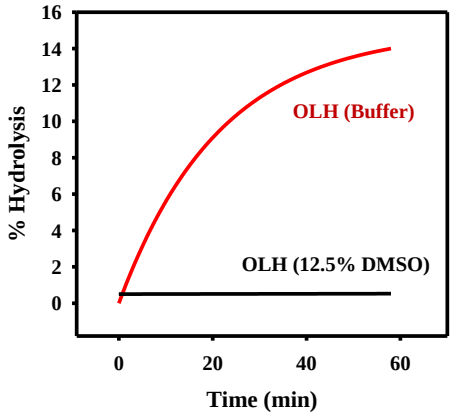

Figure S11: DMSO destabilized the micellar surface to result in the soluble monomeric amphiphile. The catalytic activity of OLH diminished in the presence of DMSO suggesting the role of self-assembly and surface formation. The initial rate of reaction decreased to ~ 0.002 $\mu mol.min^{-1}$ [data fitted to the linear equation and the slope was treated as the initial rate in the presence of DMSO (monomeric catalyst)]. The prebiotic self-assembly of the catalyst (OLH) increased the rate by ~ 1000-fold.

Prebiotic synthetic route of N-lauroyl aspartic acid (NLA):

We performed a dry-down reaction with L-aspartic acid and lauric acid (1:1 mixture, 40 mM each) in pH 3.0 buffer at 90 ^{o}C at atmospheric pressure. After two wet-dry cycles at 90 ^{o}C over a period of 24 hours, we checked the mass spectrum of the reaction mixture. We observed the corresponding amide (NLA) peak at m/z $[M-H]^+$ = 316.2136 (expected m/z = 316.2124). We synthesized NLA by general protection and deprotection method **(see the synthetic procedure of NLA),** and we found the mass of the synthesized compound is $[M-H]^+$ = 316.2115. The presence of 1675 cm^{-1} peak suggests the presence of an amide bond (**Figure S12**).

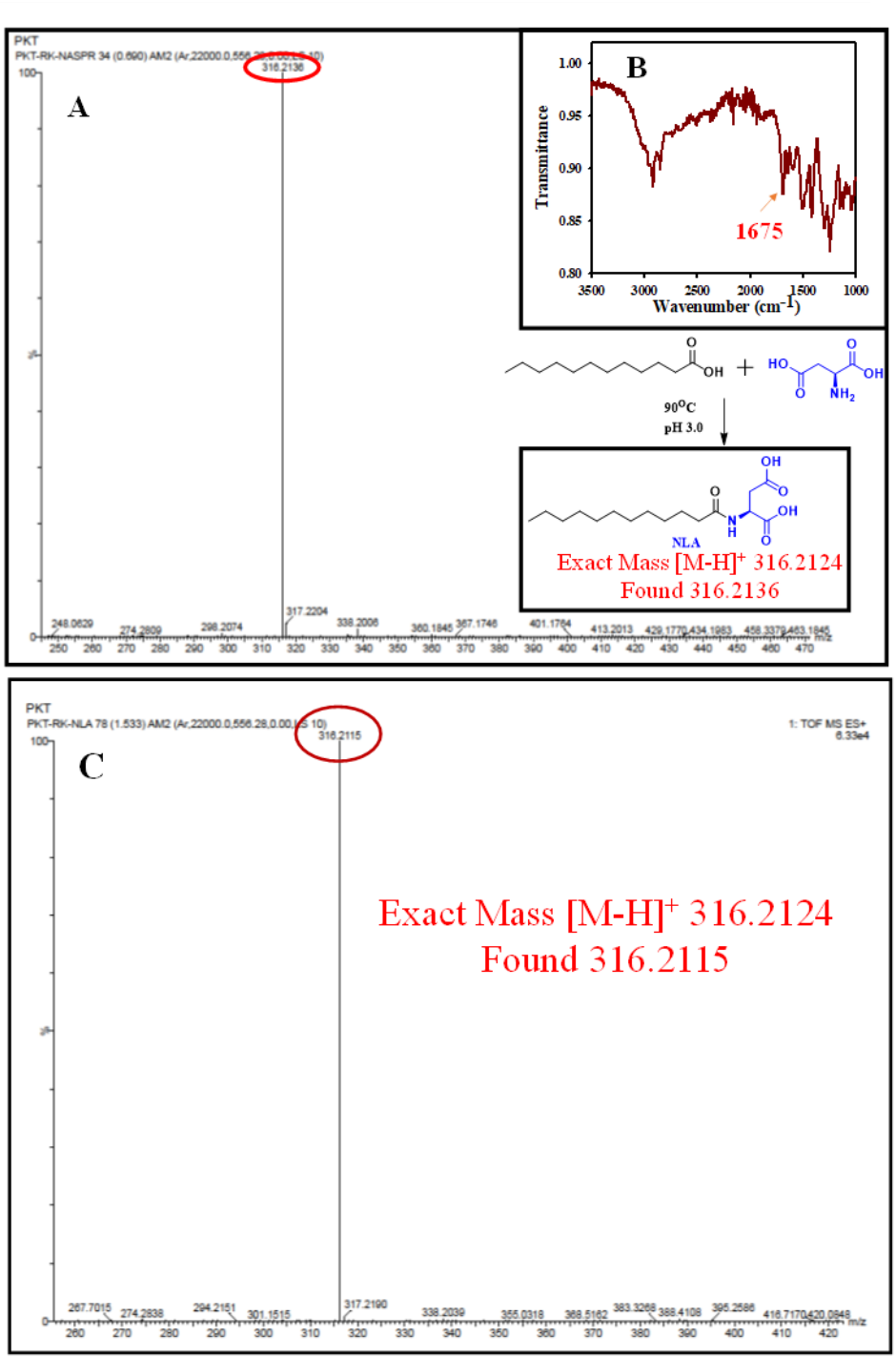

Figure S12: Detection of NLA by mass and IR spectra. A) Detection of NLA by mass from dry-down reactions with L-aspartic acid and lauric acid. B) IR spectra of the dry-down reaction mixture of L-aspartic acid and lauric acid. C) Mass spectra of synthesized NLA.

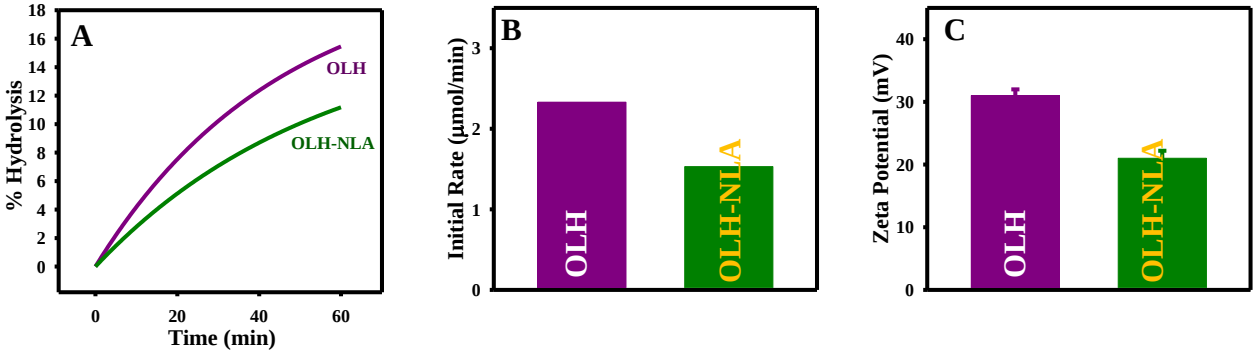

Figure S13: Esterase activity of OLH in the presence of NLA. A, B) Catalytic activity of OLH in the presence of NLA. C) Zeta potential decreases in presence of NLA.

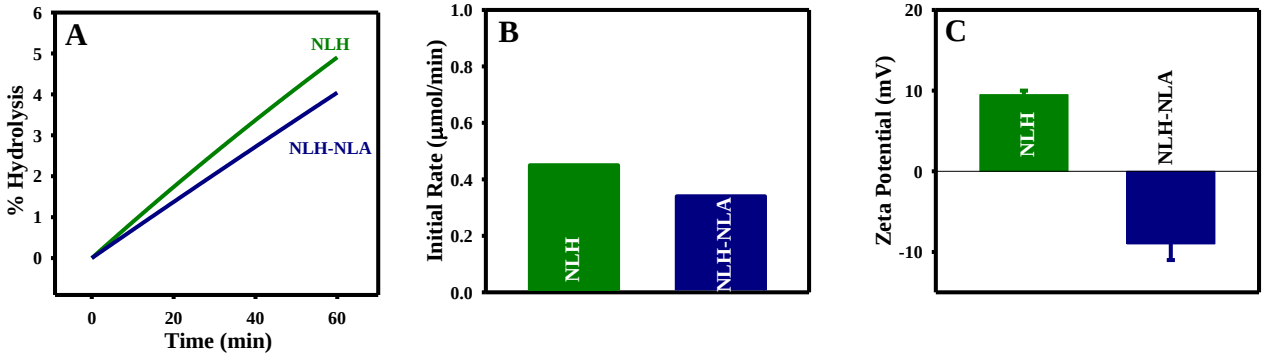

Figure S14: Esterase activity of NLH in presence of NLA. A, B) Catalytic activity of NLH in presence of NLA. C) Zeta potential decreases in presence of NLA.

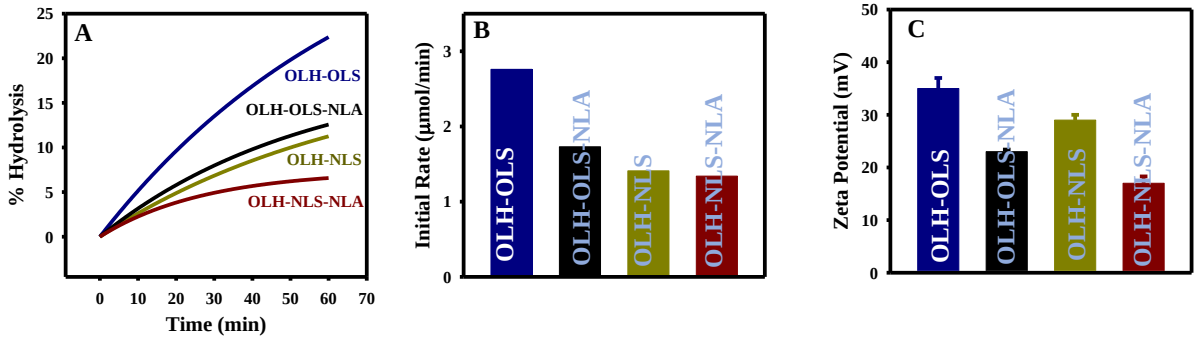

Figure S15: Esterase activity of OLH in the presence of OLS and NLA (catalytic triad). A, B) Esterase activity of prebiotic mixtures (OLH-OLS-NLA and OLH-NLS-NLA). C) Zeta potential of the mixture. 0.1 mM of each amphiphiles were used to perform the experiments.

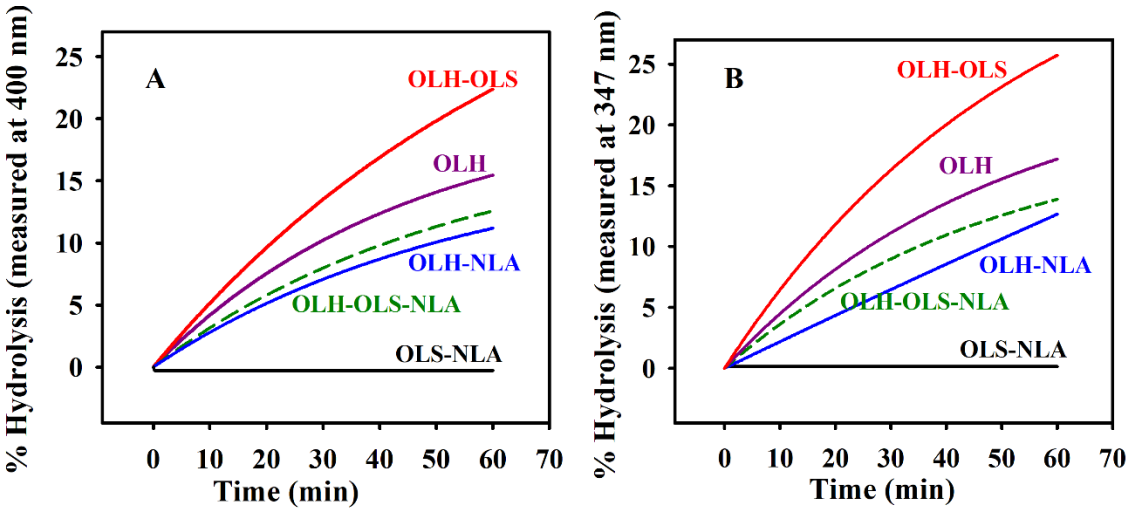

Figure S16: Hydrolytic activity of prebiotic histidine-based, serine-based and aspartic acid-based amphiphiles. A) Release of *p*-nitrophenol monitored at 400 nm, B) Release of *p*-nitrophenol monitored at 347 nm. Concentration of each amphiphiles were 0.1 mM. The experiments were performed at pH 7.0, 25 ^{o}C. Dash line (---) corresponds to OLH-OLS-NLA surface.

Surface charge (CTAB, SDBS) tunes the catalytic efficiency of OLH: 0.5 mM butyl- *p*-nitro phenol (BP) was dissolved at pH 7.0, 20 mM tris buffer. 2 mM micelle (CTAB, SDBS) was added to the substrate. Then 0.1 mM OLH was added to the micellar solution and the absorbance was recorded at 400 nm in a Biotek microplate reader. Then % of hydrolysis was calculated by using the molar extinction coefficient value of *p*-nitro phenol.

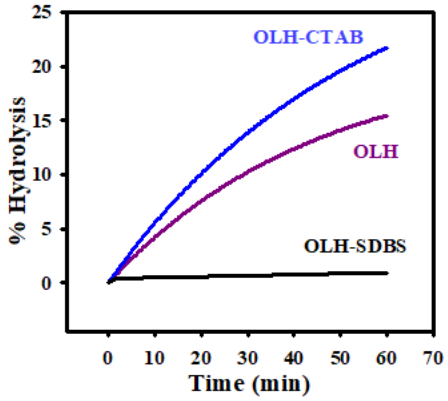

Figure S17: Micellar surface charge tune the catalytic efficiency of OLH. The initial rate (a*b) of OLH-CTAB was calculated by fitting the kinetic curve (product concentration vs time) to the mono-exponential equation ($y = a(1 - e^{-bx}$). The initial rate of OLH-SDBS was calculated by fitting the kinetic curve to the linear equation (y=ax). The initial rate of reaction

in the cationic surface (~3.0 µmol/min) decreased to ~ 0.045 µmol/min in the anionic surface, suggesting that the surface can modulate the rate by ~ 65-fold.

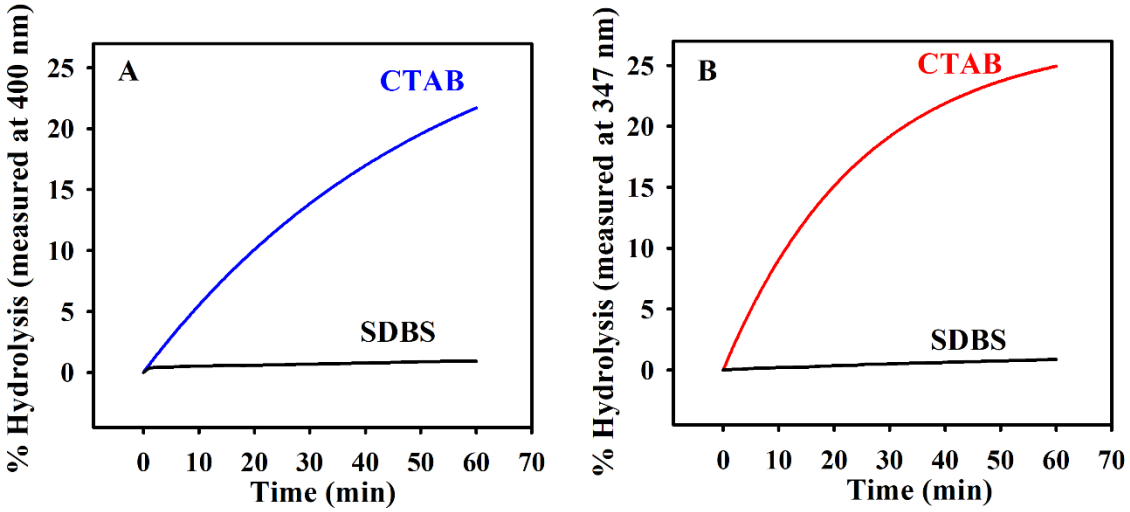

Figure S18: Micellar surface charge tune the catalytic efficiency of OLH. A) Release of *p*-nitrophenol monitored at 400 nm, B) Release of *p*-nitrophenol monitored at 347 nm.

In-situ modulation of surface charge to control the catalysis of OLH: Here we used various surfaces (Triton X-100 as neutral surface, SDBS as negative surface, and CTAB as positive surface) to check the catalytic activity of OLH. At first Triton X-100 (2 mM) was added to the 0.1 mM OLH and 0.5 mM BP solution. The kinetics of the hydrolysis was monitored as described earlier. At 15 minutes, 2 mM SDBS was added, and the kinetics was monitored again. At 30 minutes 4 mM CTAB was added and, at 45 minutes 8 mM SDBS was added in situ. The kinetics was monitored spectrophotometrically.

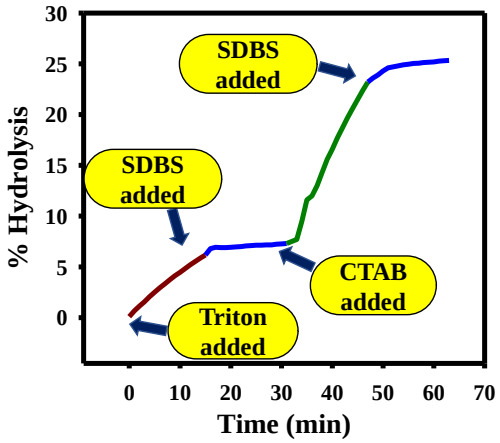

Figure S19: In-situ addition of SDBS and CTAB into OLH-Triton X-100 micelles and the hydrolytic activity.

Role of acyl chain length of catalysts and catalysis: Substrate (BP, 0.5 mM), individual catalyst (OLH, OOH, OBH and Histidine, 0.1 mM) and CTAB (2 mM) were mixed in pH 7.0

buffer. The hydrolytic ability of the catalyst was monitored at 400 nm in a Biotek microplate reader. Interestingly, only histidine (not acylated) does not exhibit any catalytic activity. The increase in the chain length of the catalyst increased the rate and extent of the hydrolysis.

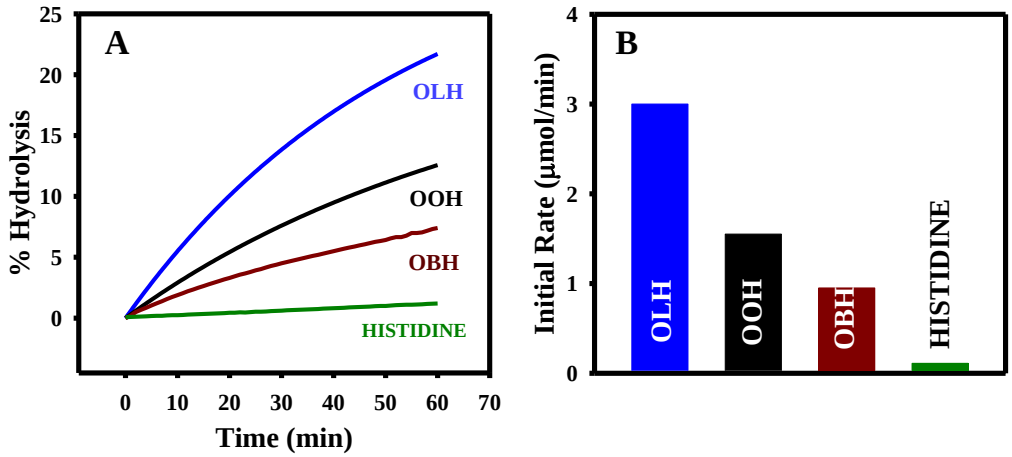

Figure S20: The role of acyl chain length of catalysts.

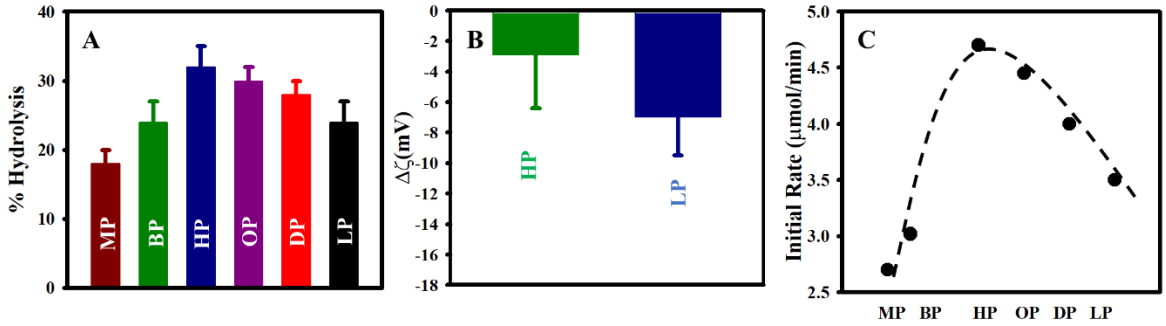

Figure S21: Substrate selectivity of the catalyst OLH. A) Role of the substrate and % hydrolysis; B) change in the zeta potential of the surface before and after hydrolysis with hexyl and lauryl ester. C) Initial rate of various type of substrates (gaussian nature).

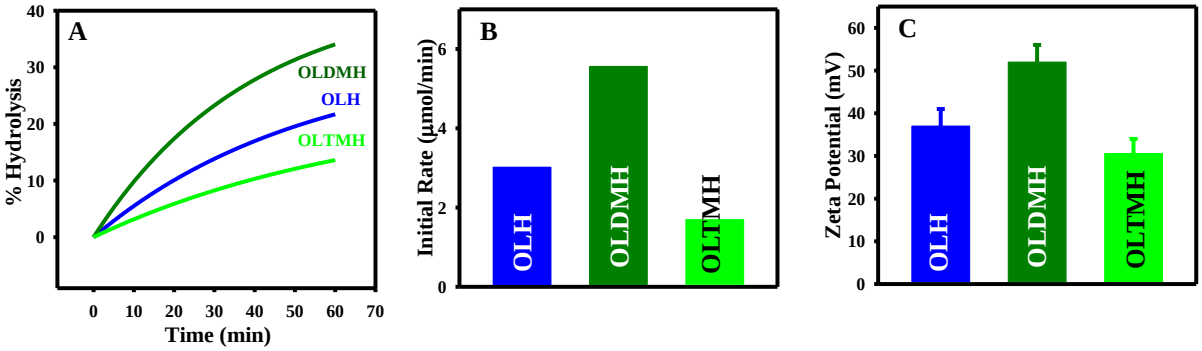

Figure S22: Methylation of histidine amine and pK_a perturbation. A) Role of methylation on the catalytic efficiency; B) the initial rate of reaction of methylation; C) the surface potential of the OLH and the methylated catalyst.

Substrate selectivity of the catalyst OLDMH and OLTMH: Various chain length substrate was used at 0.5 mM, catalysts (OLDMH and OLTMH) were used at 0.1 mM, and CTAB (2 mM) was used as an external positive surface. The reaction was monitored at 400 nm in a Biotek microplate reader.

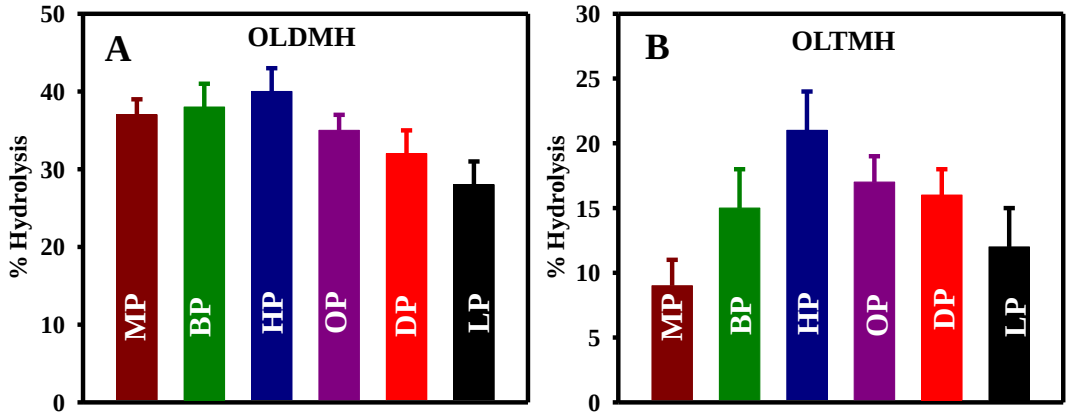

Figure S23: Substrate selectivity of the catalysts OLDMH and OLTMH.

Catalytic activity of different catalysts in presence of various surfaces (positive, negative, neutral)

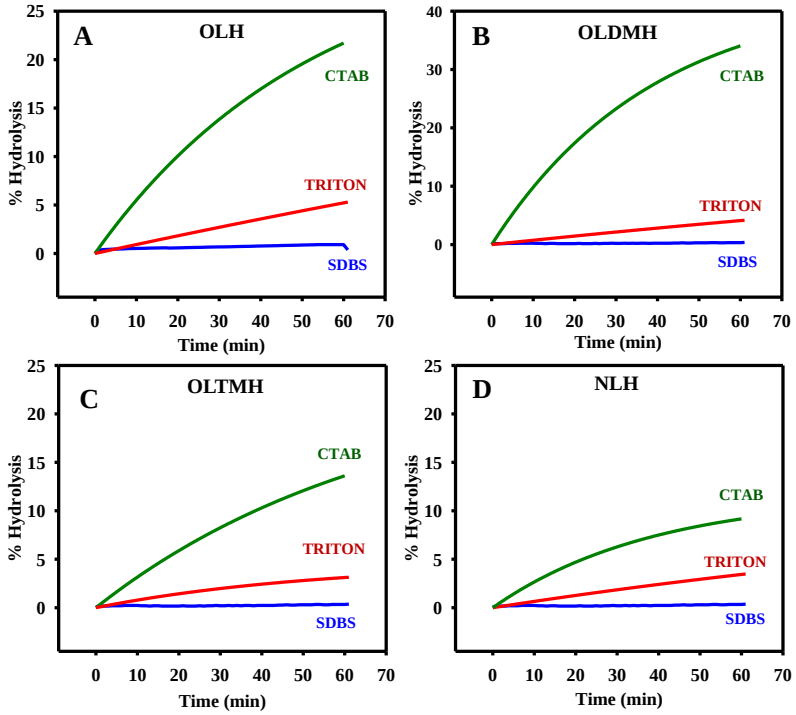

Figure S24: Catalytic activity of various catalysts at various surfaces. The initial rate (a*b) of OLDMH-CTAB (**B**) was calculated by fitting the kinetic curve (product concentration vs time) to the mono-exponential equation ($y = a(1 - e^{-bx}$). The initial rate (a) of OLDMH-SDBS was calculated by fitting the kinetic curve to the linear equation (y=ax). The initial rate of reaction in the cationic surface (~5.5 μmol/min) decreased to ~ 0.015 μmol/min in the anionic

surface, suggesting that the surface can modulate the rate by ~ 300-fold. Since the rate of monomeric OLH in DMSO was 0.002 μmol/min, we suggest that self-assembly and methylation can increase the initial rate by ~ 2500-fold.

Mechanism of hydrolysis by histidine based amphiphiles.

Detection of intermediate and nucleophilic attack by imidazole: The initial attack to the ester carbonyl might happen by either imidazole or α-amine. Since the pKa of imidazole is much lower than -NH_2, we expect that initial attack to ester might happen via imidazole nucleophile. Since OLS with only α-amine exhibited only 2-3% hydrolysis (**Figure 1B**), we ignored the effect of α-amine at such a low concentration (0.1 mM). We doubled the concentration of OLS to 0.2 mM and performed similar experiments (**Figure S25**). We found that the % hydrolysis increased to 4%, which is negligible. Also, the experiments with OLH and OLDMH suggest that OLDMH behaved as a better catalyst (**Figure 4D**). The α-amine of OLDMH is a tertiary one and cannot assist nucleophilic attack. Therefore, we believe that at our experimental conditions, the effect of nucleophilic attack via α-amine is minimal.

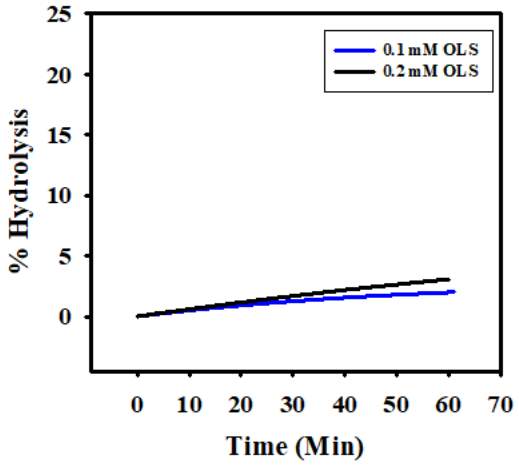

Figure S25: Hydrolytic activity of OLS by α-amine.

To identify the intermediate formation via the attack of imidazole nucleophile, we performed HRMS of the reaction mixture. Reactions were kept with 0.1 mM OLH/OLTMH and 0.5 mM BP in 2 mM CTAB surface at pH 7.0. After 30 minutes, small aliquot was taken and HRMS was recorded immediately. We identified the activated quaternary amide intermediate in HRMS (**Figures S26-27**).

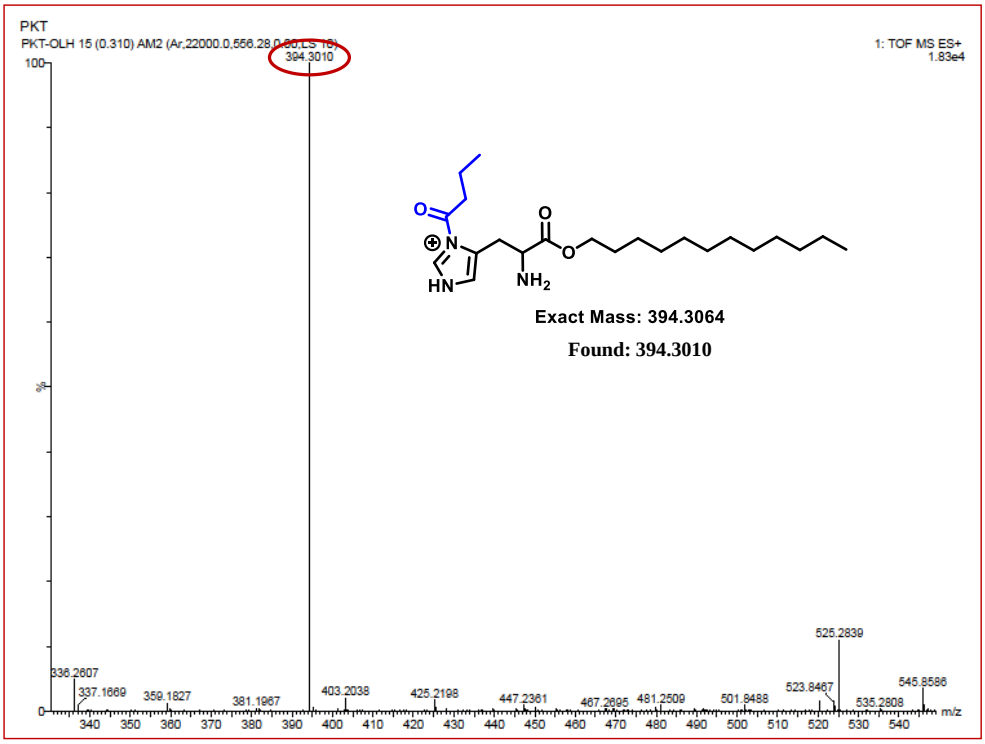

Figure S26: HRMS of activated quaternary amide intermediate of OLH and BP.

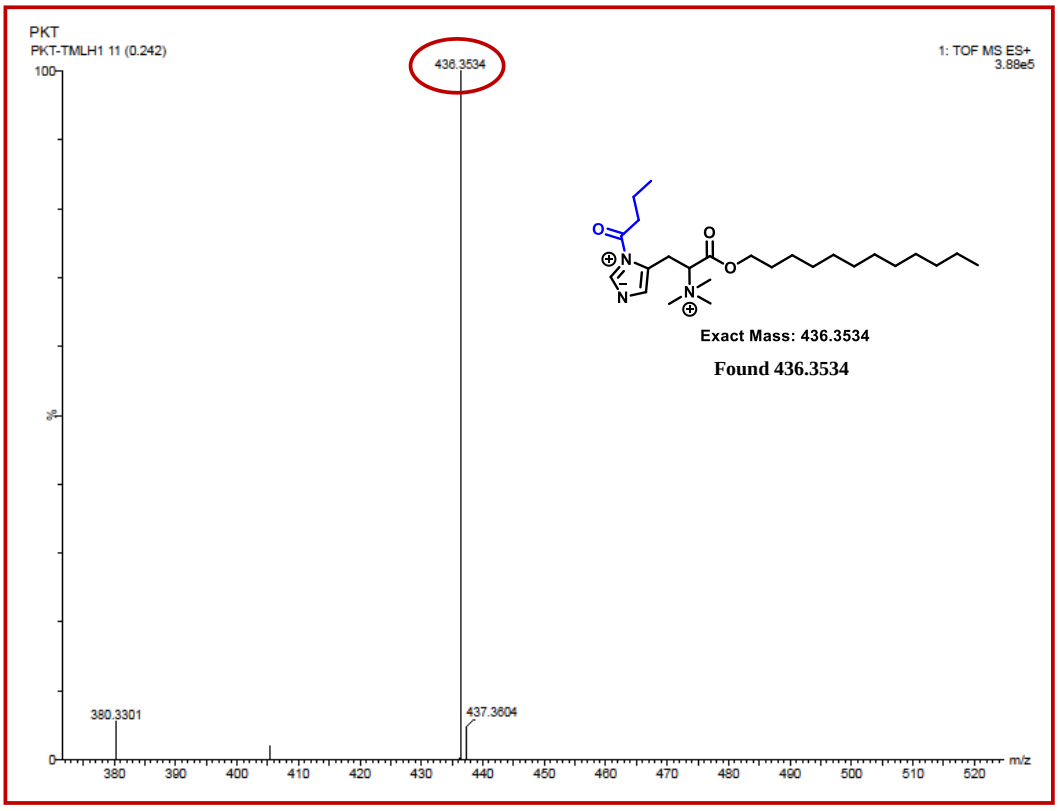

Figure S27: HRMS of activated quaternary amide intermediate of OLTMH and BP.

Probable Mechanism: After the intermediate formation via nucleophilic attack by imidazole, the activated quaternary amide intermediate will be hydrolyzed to products and the catalyst will be regenerated.

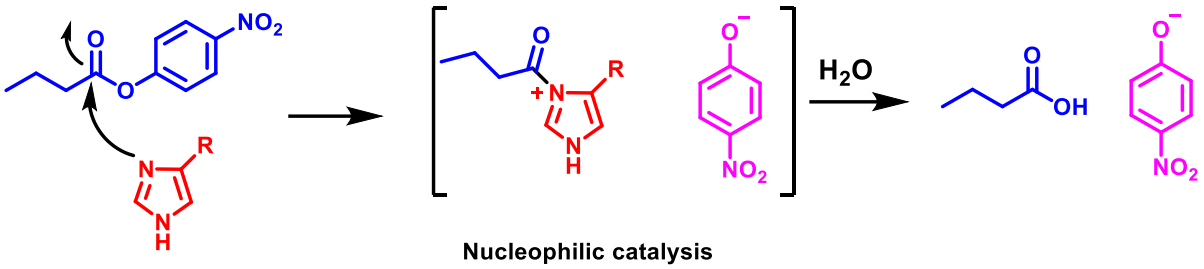

Figure S28: Probable mechanism of hydrolysis.

Determination of kinetic parameters of OLH, OLDMH and OLTMH in CTAB surface: We performed kinetic experiments at various substrate concentrations. In the presence of a catalytic amount of OLH, the initial rate of hydrolysis linearly increased at low substrate concentration, and then non-linearity was noticed at high substrate concentration. The kinetics parameters can be determined by the Michaelis Menten equation. The turnover rate (k_{cat}) was calculated to be 0.14 min^{-1} OLH. Notably, OLH showed a catalytic efficiency (k_{cat}/K_M) of 241 $M^{-1}min^{-1}$, which is comparable with previously reported systems (**Table S1**).

Table S1: Kinetics parameters of OLH, OLDMH, and OLTMH catalysts and comparison of the parameters with reported catalytic systems.

Sl No.	Catalysts	k_{cat}/K_M ($M^{-1}min^{-1}$)	k_{cat} (min^{-1})	K_M (mM)	References
1	OLH	241	0.14	0.58	Present work
2	OLDMH	344	0.165	0.48	Present work
3	OLTMH	61	0.09	1.48	Present work
4	Enzyme-inspired catalyst (R8)	136	1.63	12	Connal et al.[2]
5	ACT surfactant	187	198	1061	Connal et al.[3]
6	ACT-C16/CTAB/ Guan-C16	77551	114	1.47	Connal et al.[4]
7	$Q11HR_{max}$	9	0.16	17.63	Zhang et al.[5]

8	Aggregated AM1	53	0.076	1.43	Gayen et al.[6]
9	Peptide amphiphiles immobilized onto silica nanoparticle	11	0.068	6.4	Das et al.[7]
10	Hydrogelator 1	315	1.26	4.0	Singh et al.[8]
11	Peptide amphiphile	2500	1.0	0.4	Stupp et al.[9]
12	PSACT Nanocatalyst	1325	0.53	0.4	Wang et al.[10]

Dynamic light scattering: Zeta potential of various surfaces was monitored by dynamic light scattering (DLS), Malvern Zetasizer Nano ZS (Malvern Instruments Ltd., UK) equipped with a He-Ne laser (wavelength: 633 nm).

Synthetic procedures: Compound 3 (OLH):

Procedure 1:

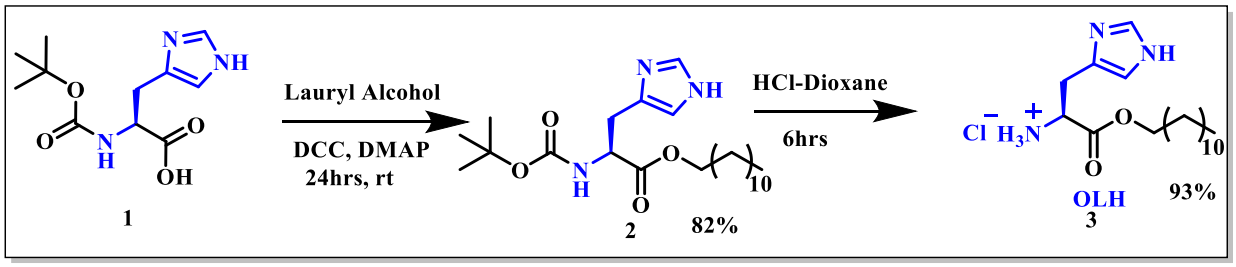

Boc-Histidine **1** (500mg, 1.96 mmol) was dissolved in dry DCM (10 ml). Then DCC (484.5 mg, 2.352 mmol), DMAP (47.82 mg, 0.392 mmol), and lauryl alcohol (401 mg, 2.156 mmol) were added to the reaction mixture, and the reaction mixture was stirred for 24 hrs at room temperature. After completion of the reaction, the reaction mixture was concentrated under reduced pressure and dissolved in ethyl acetate (EtOAc) and filtered to remove DCU. The filtrate was concentrated under reduced pressure, and the residue (890 mg) was purified by flash chromatography (EtOAc/Hexane 4:1) to give pure compound **2** (705 mg, 82%) as colourless gum liquid. Compound **2** was dissolved in dry HCl-Dioxane (~ 4M) and stirred for 6 hrs. Then diethyl ether was added and resulted solid was filtered and dried in a vacuum desiccator to get pure compound **3** (540 mg, 93%); ^{1}H NMR (500 MHz, DMSO) δ 9.10 (s, 1H), 7.53 (s, 1H), 4.49 (t, *J* = 7.2 Hz, 1H), 4.16 – 4.02 (m, 2H), 3.32 (dd, *J* = 7.1, 2.8 Hz, 2H), 1.50 (m, 2H), 1.23 (m, 18H), 0.84 (t, *J* = 6.8 Hz, 3H). ^{13}C NMR (126 MHz, DMSO) δ 168.11,

133.87, 126.78, 117.95, 65.85, 50.95, 31.26, 30.20, 29.03, 29.00, 28.95, 28.89, 28.69, 28.61, 27.79, 25.08, 22.06, 13.91.

HRMS [ESI]: $[M+H]^+$ Found: 324.2648, $C_{18}H_{34}N_3O_2$ requires 324.2651. The ^{1}H-NMR peak positions of a-c, e (aromatic and near-aromatic protons) were dependent on the protonation status of imidazolium and ammonium groups (see below).

^{1}H-NMR of compound 3 (OLH): Fully protonated in presence of 4 M HCl-Dioxane.

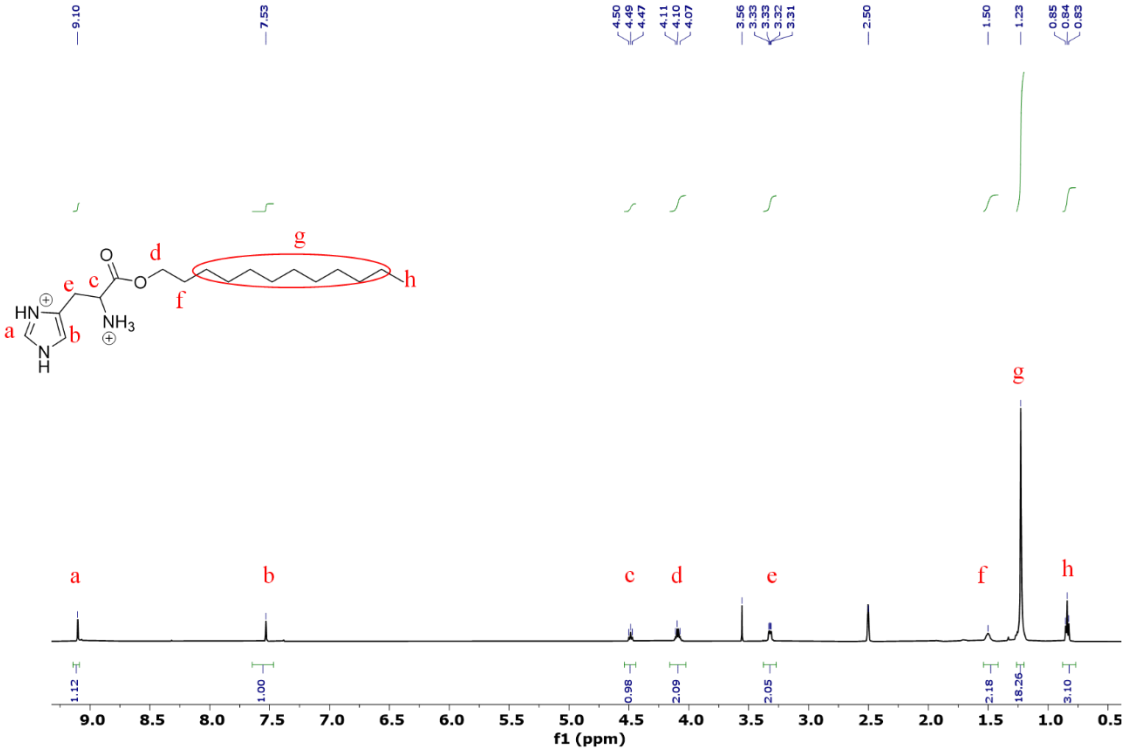

^{13}C-NMR of compound 3 (OLH):

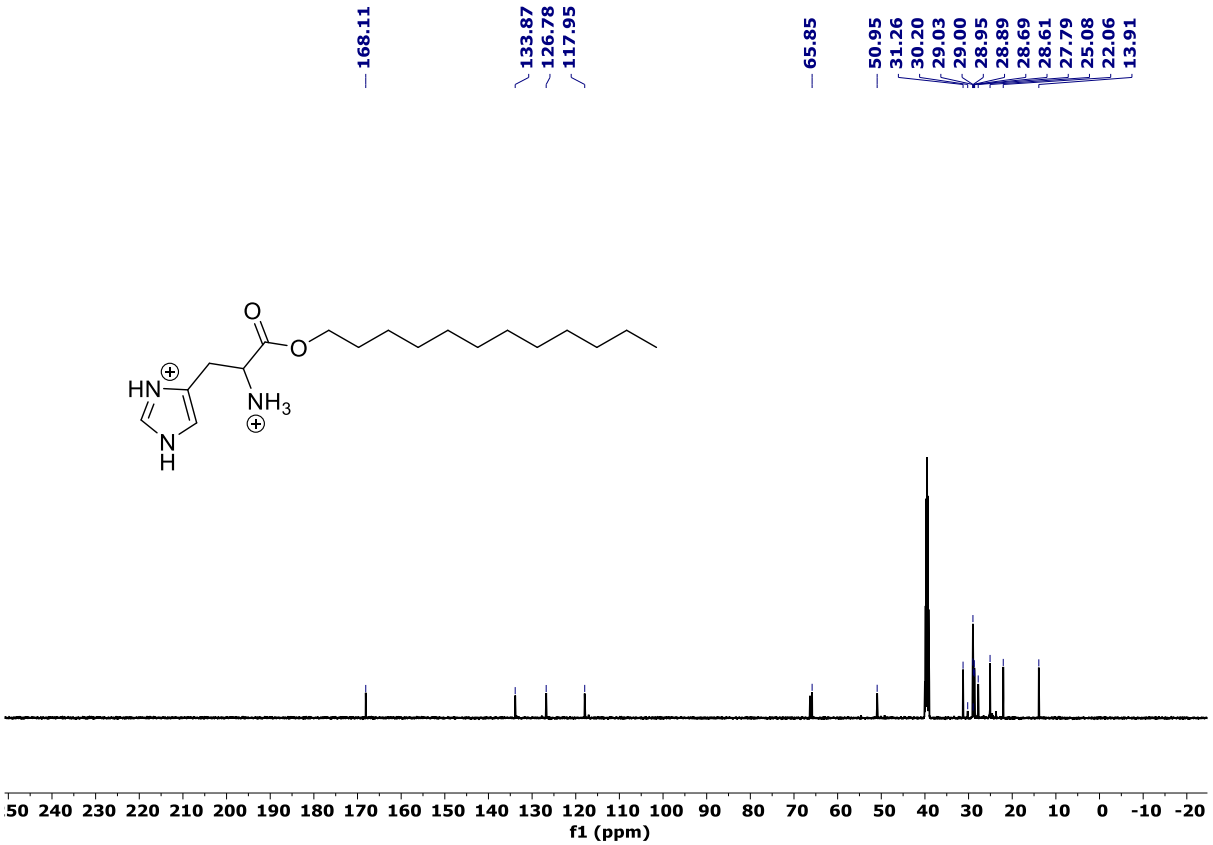

^{1}H-NMR of compound 3 (OLH): Partially protonated/deprotonated in presence of $NaHCO_3$.

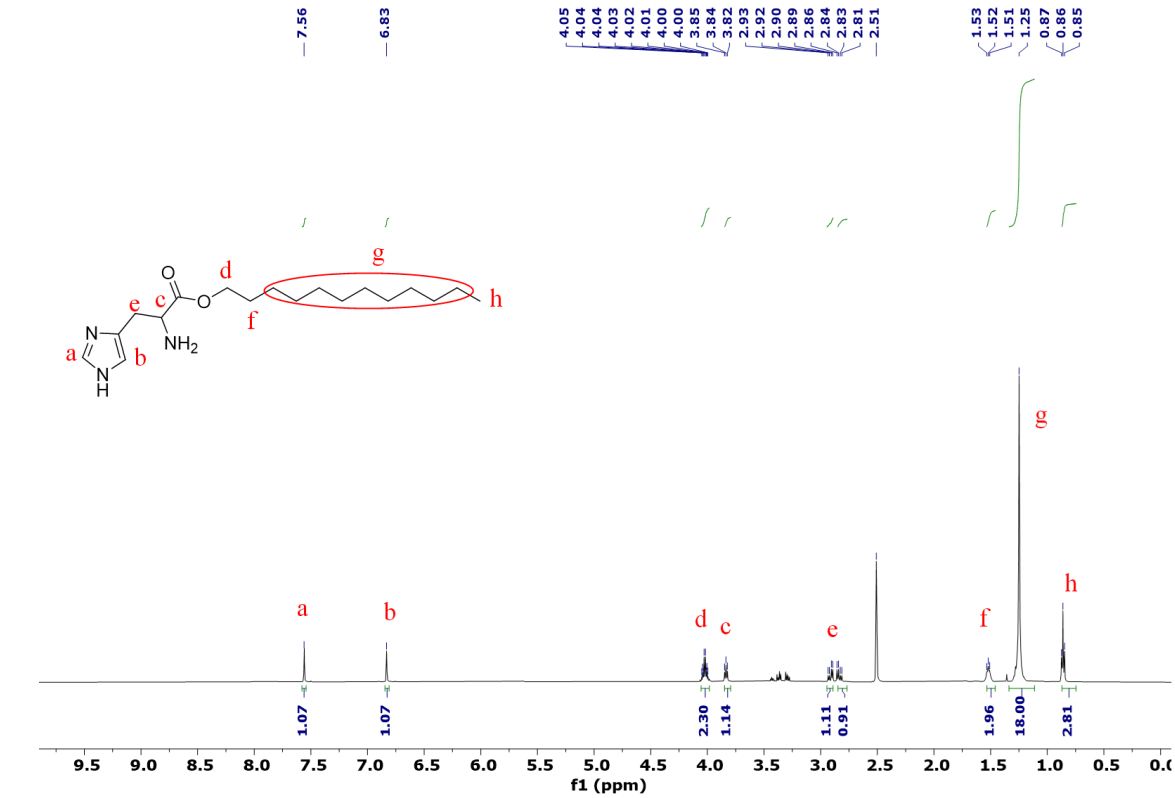

Compound 5 (OLDMH):

Procedure 2:

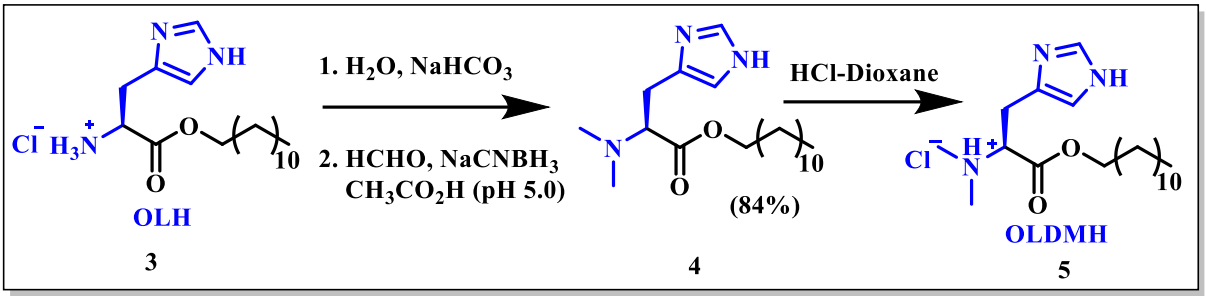

Compound **3** (360 mg, 0.5 mmol) was dissolved in water (10 ml). Then $NaHCO_3$ was added to neutralize the compound, and the resulting solid compound was dissolved in CH_3CN (10 ml). Then 37-40% HCHO solution (1 ml, ~12 mmol) and $NaCNBH_3$ (503 mg, 8 mmol) was added to the reaction mixture. Acetic acid was added immediately to adjust the pH to 5.0. Then the reaction mixture was stirred for 1 hr at room temperature. After completion of the reaction, the reaction mixture was concentrated under reduced pressure and the residue (960 mg) was purified by flash chromatography (MeOH/DCM 1:20) to give pure compound **4** (301 mg, 84%) as colourless gum liquid. Compound **4** was dissolved in dry HCl-Dioxane (~4M) and stirred for 2 hrs. Then diethyl ether was added and resulted semi-solid compound **5** was concentrated under reduced pressure. ^{1}H NMR (400 MHz, DMSO-D_6) δ 9.11 (s, 1H), 7.55 (s, 1H), 4.68 (dd, J = 9.5, 5.3 Hz, 1H), 4.08 (t, J = 6.7 Hz, 2H), 3.52 (d, J = 5.3 Hz, 1H), 3.37 (dd, J = 15.1, 10.1 Hz, 1H), 2.87 (s, 6H), 1.57 – 1.40 (m, 2H), 1.39 – 1.02 (m, 18H), 0.85 (t, J = 4.6 Hz, 3H). ^{13}C NMR (126 MHz, DMSO) δ 166.68, 134.04, 127.08, 117.59, 66.35, 64.14, 40.83, 31.29, 29.03, 28.88, 28.71, 28.57, 28.54, 27.61, 27.57, 25.10, 22.14, 22.08, 13.92. HRMS [ESI]: $[M+H]^+$ Found: 352.2960, $C_{20}H_{38}N_3O_2$ requires 352.2964.

^{1}H-NMR of compound 5 (OLDMH):

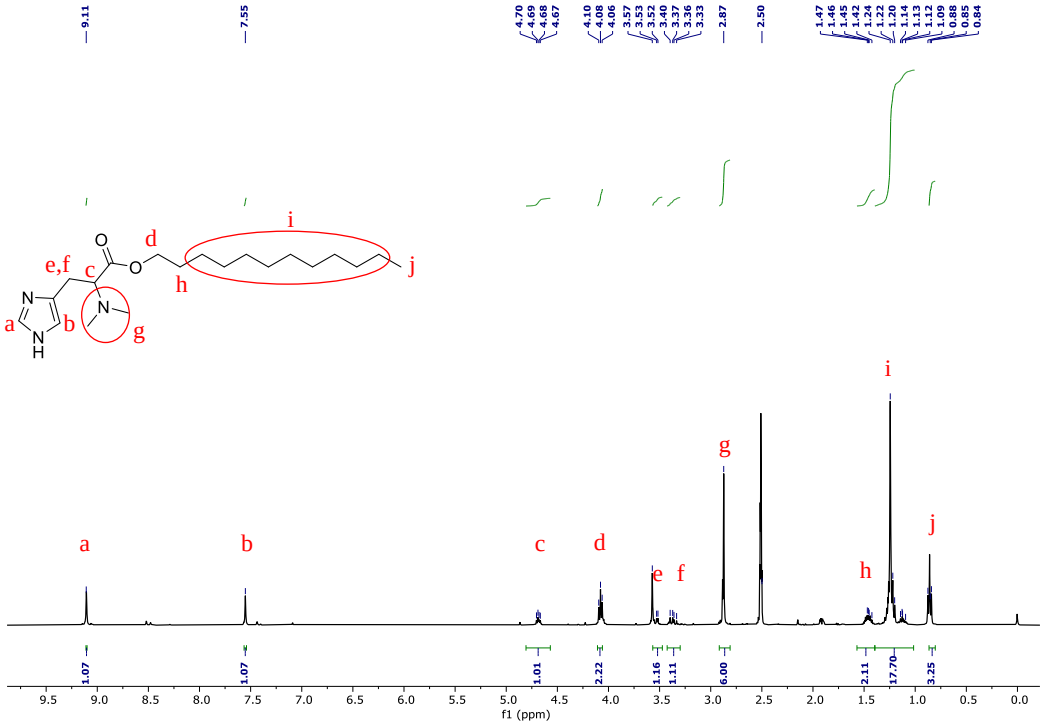

^{13}C-NMR of compound 5 (OLDMH):

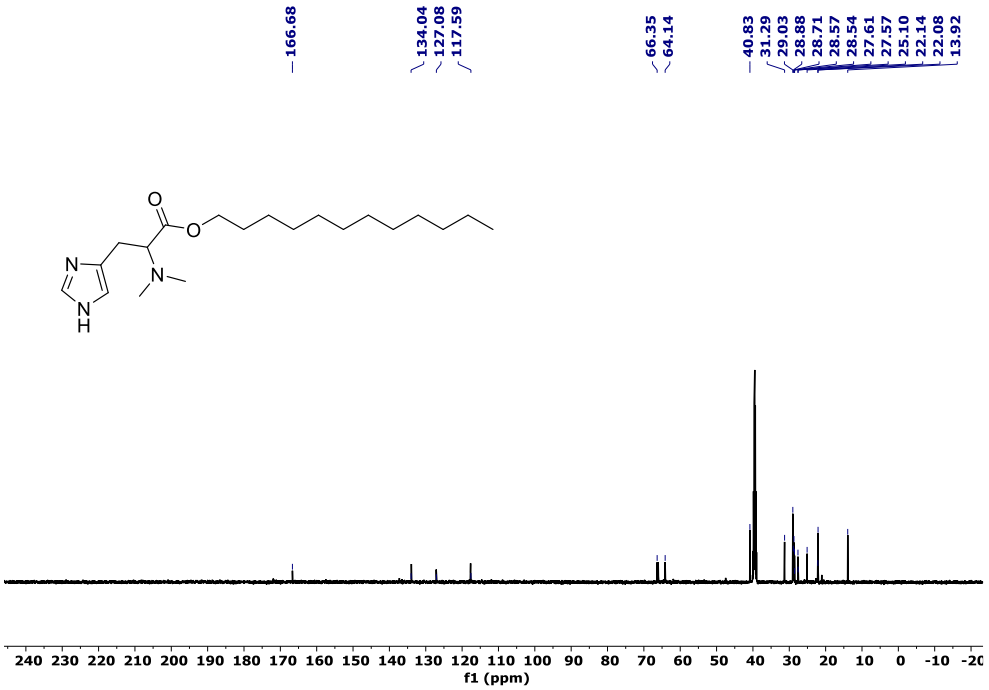

Compound 6 (OLTMH):

Procedure 3:

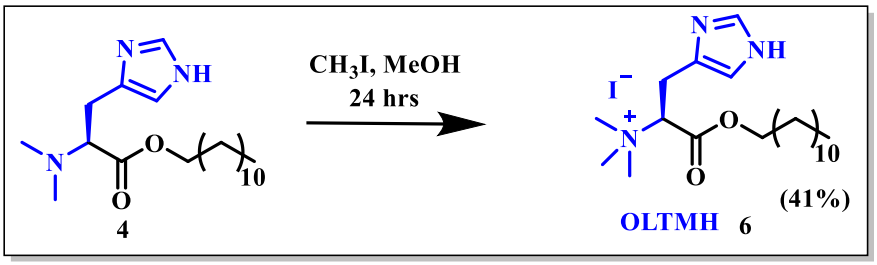

Compound **4** (100 mg, 0.28 mmol) was dissolved in MeOH and added CH_3I (60 mg, 0.42 mmol) and stirred the reaction mixture for 24 hrs. Then the reaction mixture was concentrated under reduced pressure and the residue (120 mg) was purified by flash chromatography (MeOH/DCM 1:20) to give pure compound **6** (58 mg, 41%) as colourless gum liquid. ^{1}H NMR (500 MHz, DMSO) δ 7.58 (s, 1H), 6.94 (s, 1H), 4.53 (dd, *J* = 11.2, 2.9 Hz, 1H), 4.04 (t, *J* = 6.5 Hz, 2H), 3.24 (m, 11H), 1.46 – 1.39 (m, 2H), 1.24 (m, 18H), 0.85 (t, *J* = 7.1 Hz, 3H); ^{13}C NMR (126 MHz, DMSO) δ 167.33, 135.89, 133.17, 114.58, 73.85, 66.35, 52.12, 31.69, 29.42, 29.41, 29.38, 29.27, 29.10, 28.92, 27.90, 26.06, 25.45, 22.48, 14.34. HRMS [ESI]: $[M]^+$ Found: 366.3126, $C_{21}H_{40}N_3O_2$ exact mass 366.3115.

^{1}H-NMR of compound 6 (OLTMH):

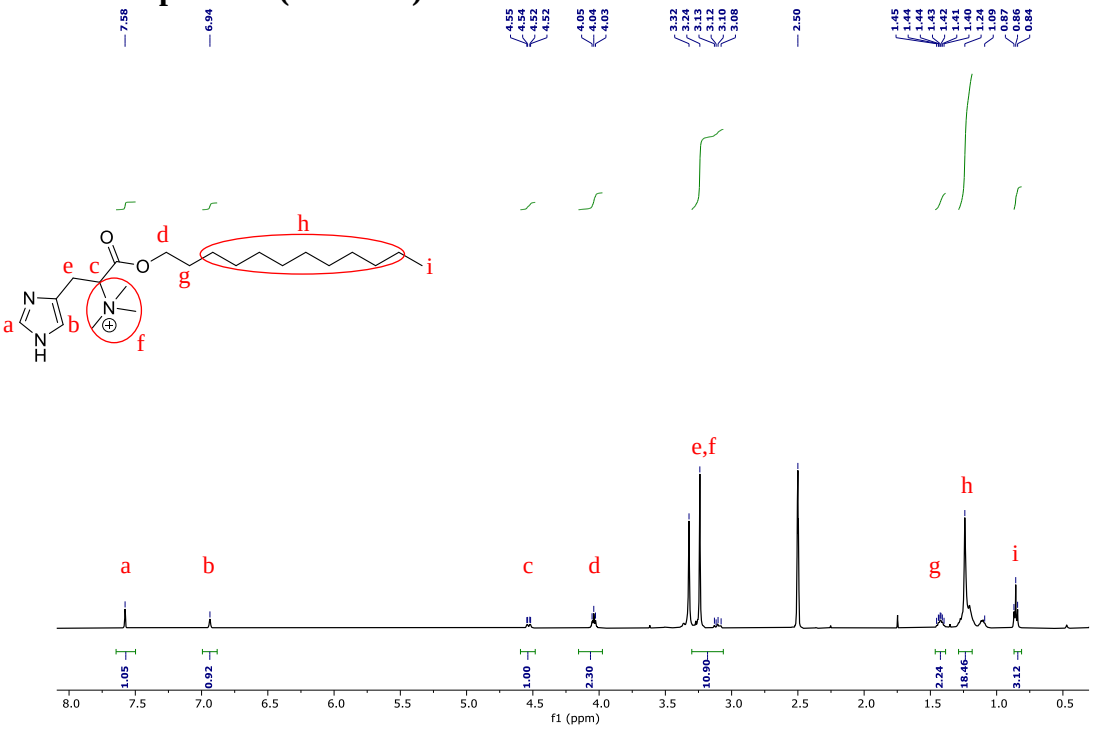

^{13}C-NMR of compound 6 (OLTMH):

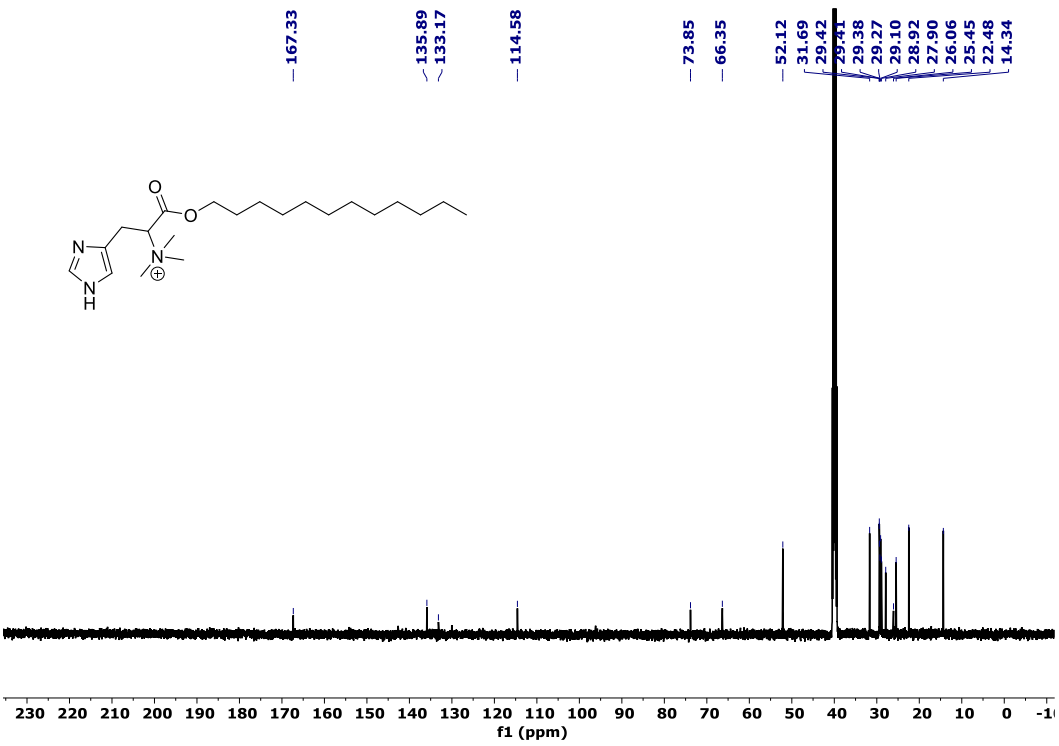

Compound 8 (NLH):

Procedure 4:

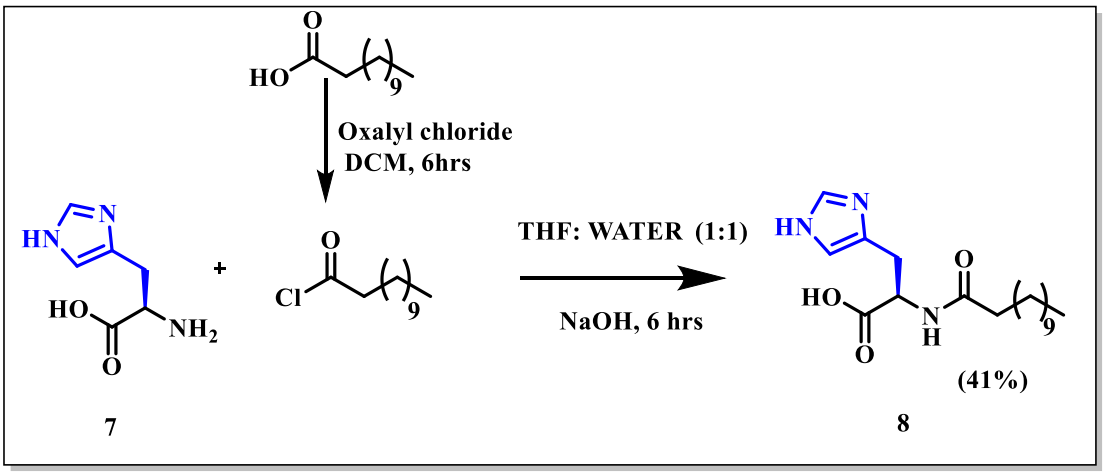

L-Histidine **7** (1 g, 6.5 mmol) and NaOH (0.4 g, 7.2 mmol) were dissolved in 30 ml water and 10 ml THF mixed solvent, and the solution was stirred for 10 minutes. Fresh lauroyl chloride was synthesized from lauric acid and 4 equivalent oxalyl chloride. lauroyl chloride (1.32 g, 6.0 mmol) in 50 ml THF was added to the histidine solution slowly. After rigorously stirring for 6 hours, the solution was evaporated to remove THF. The aqueous layer was extracted by diethyl ether three times to remove the residual dodecanoyl chloride. Then the pH was adjusted to 5.0. The resulting precipitate was filtrated and washed with distilled water three times. The product **8** was dried in vacuum. A white solid powder was obtained in 45 % yield (980 mg). ^{1}H NMR (500 MHz, DMSO) δ 8.05 (d, *J* = 7.8 Hz, 1H), 7.77 (s, 1H), 6.86 (s, 1H), 4.40 (dq, *J* = 8.4, 4.7

Hz, 1H), 2.98 (dd, *J* = 14.8, 5.1 Hz, 1H), 2.86 (dd, *J* = 14.9, 8.7 Hz, 1H), 2.06 (t, *J* = 7.5 Hz, 2H), 1.43 (q, *J* = 9.8, 7.2 Hz, 2H), 1.22 (m, 16H), 0.83 (t, *J* = 6.9 Hz, 3H). ^{13}C NMR (126 MHz, DMSO) δ 173.32, 172.08, 134.35, 132.61, 117.19, 52.30, 35.19, 33.78, 31.32, 29.07, 29.03, 28.97, 28.74, 28.58, 25.21, 24.54, 22.10, 13.92. HRMS [ESI]: $[M+H]^+$ Found: 338.2424, $C_{18}H_{32}N_3O_3$ requires 338.2444.

^{1}H-NMR of compound (NLH) 8:

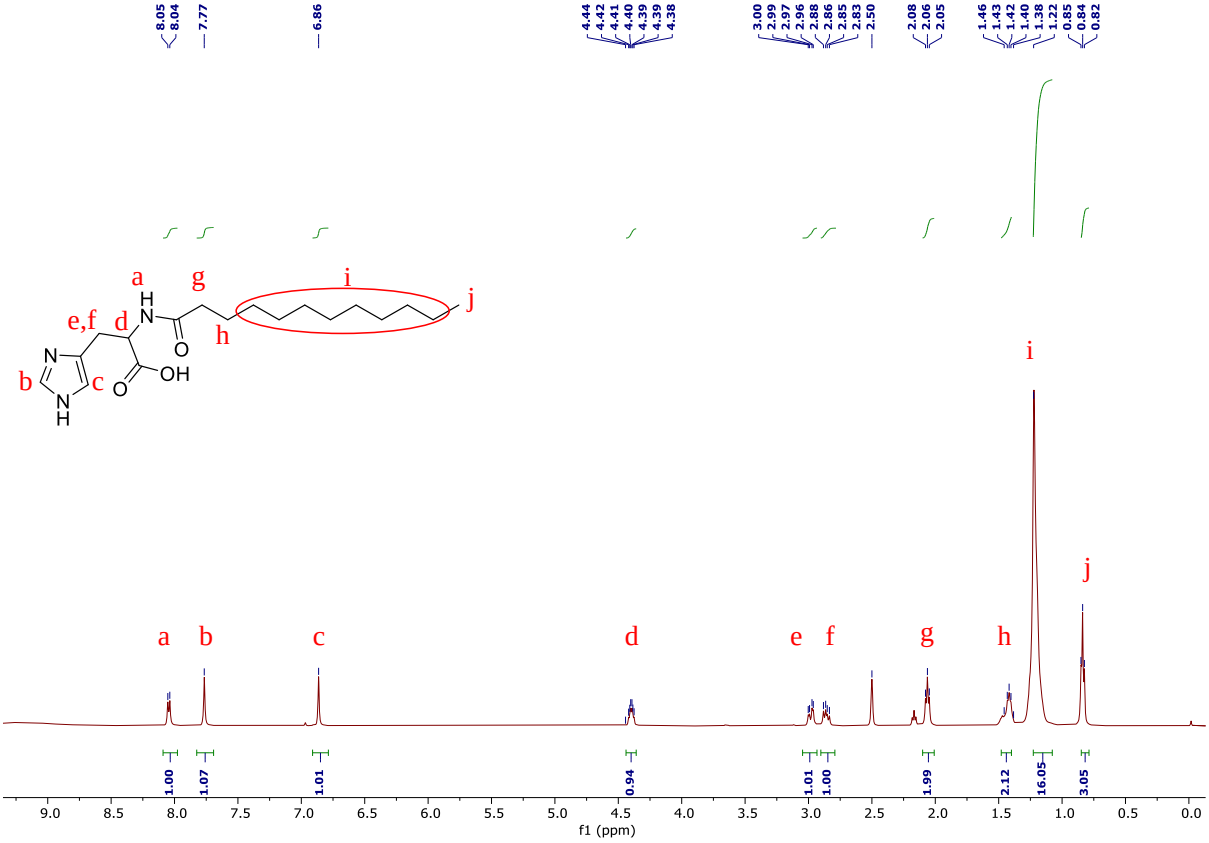

^{13}C-NMR of compound (NLH) 8:

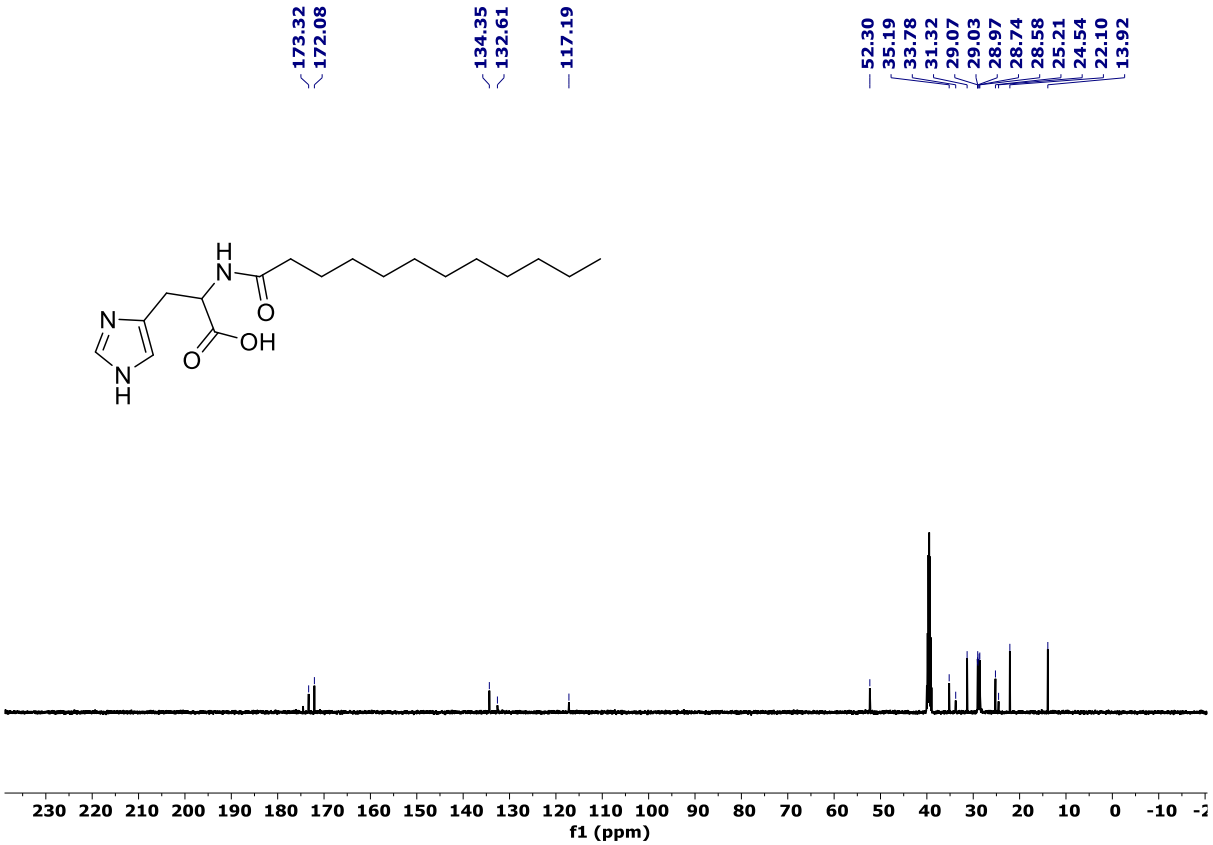

Butyl-histidine **10** and octyl histidine **9** was synthesized by using butanol and octanol by same procedure (procedure **1)**.

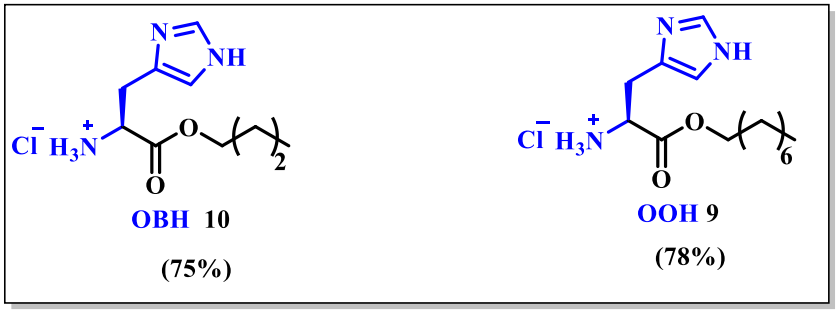

Compound 9 (OOH):

^{1}H NMR (500 MHz, DMSO) δ 9.09 (s, 1H), 7.53 (s, 1H), 4.48 (t, *J* = 7.3 Hz, 1H), 4.10 (m, 2H), 3.31 (d, *J* = 7.3 Hz, 2H), 1.51 (m, 2H), 1.24 (m, 10H), 0.86 (t, *J* = 6.9 Hz, 3H); ^{13}C NMR (126 MHz, DMSO) δ 168.15, 133.94, 126.80, 117.97, 65.89, 50.97, 31.21, 28.56, 28.53, 27.80, 25.12, 25.08, 22.05, 13.94. HRMS [ESI]: $[M+H]^+$ Found: 268.2093, $C_{14}H_{26}N_3O_2$ requires 268.2025.

Compound 10 (OBH): ^{1}H NMR (400 MHz, DMSO-*D*$_6$) δ 9.05 (s, 1H), 7.52 (s, 1H), 4.45 (t, *J* = 7.3 Hz, 1H), 4.13 (t, *J* = 6.4 Hz, 2H), 3.27 (d, *J* = 7.2 Hz, 2H), 1.55 – 1.45 (m, 2H), 1.25 (dq, *J* = 14.7, 7.4 Hz, 2H), 0.87 (t, *J* = 7.5 Hz, 3H); ^{13}C NMR (101 MHz, DMSO-*D*$_6$) δ 168.74,

134.57, 127.35, 118.52, 66.88, 51.51, 30.36, 25.70, 18.88, 14.02. $[M+H]^+$ Found: 212.1372, $C_{10}H_{18}N_3O_2$ requires 212.1399.

^{1}H-NMR of compound 9 (OOH):

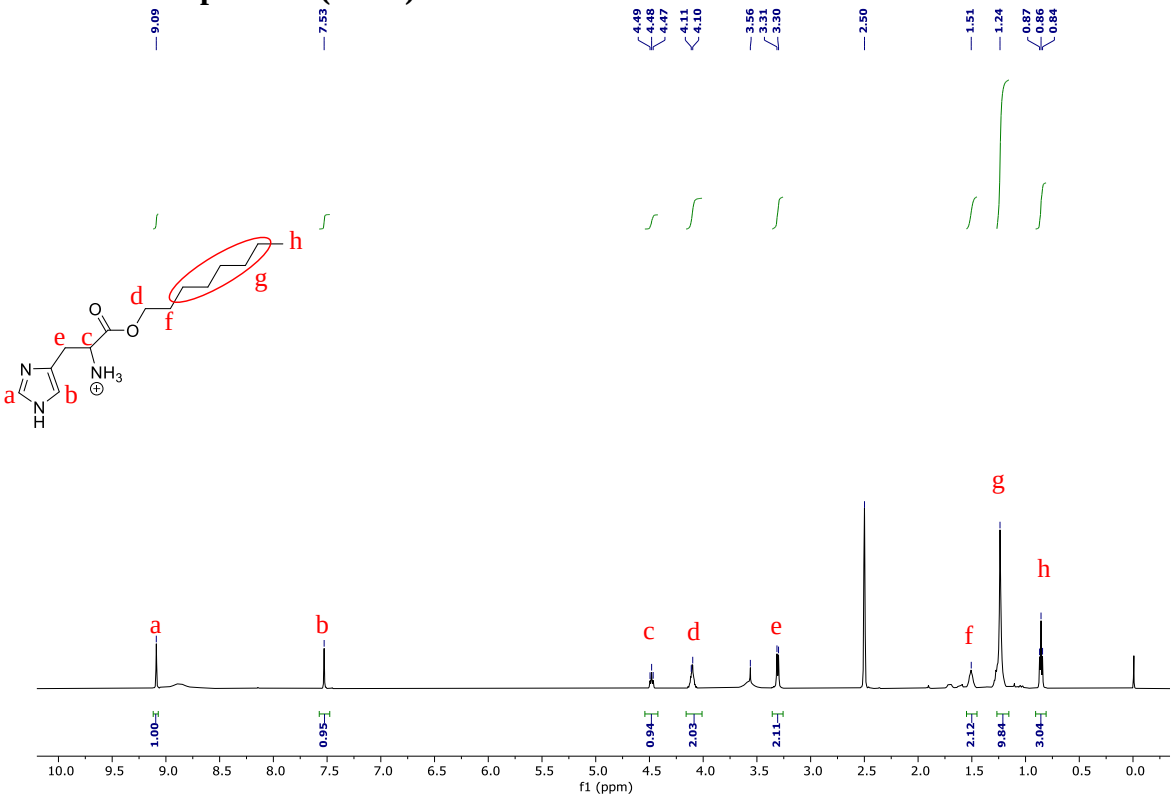

^{13}C-NMR of compound 9 (OOH):

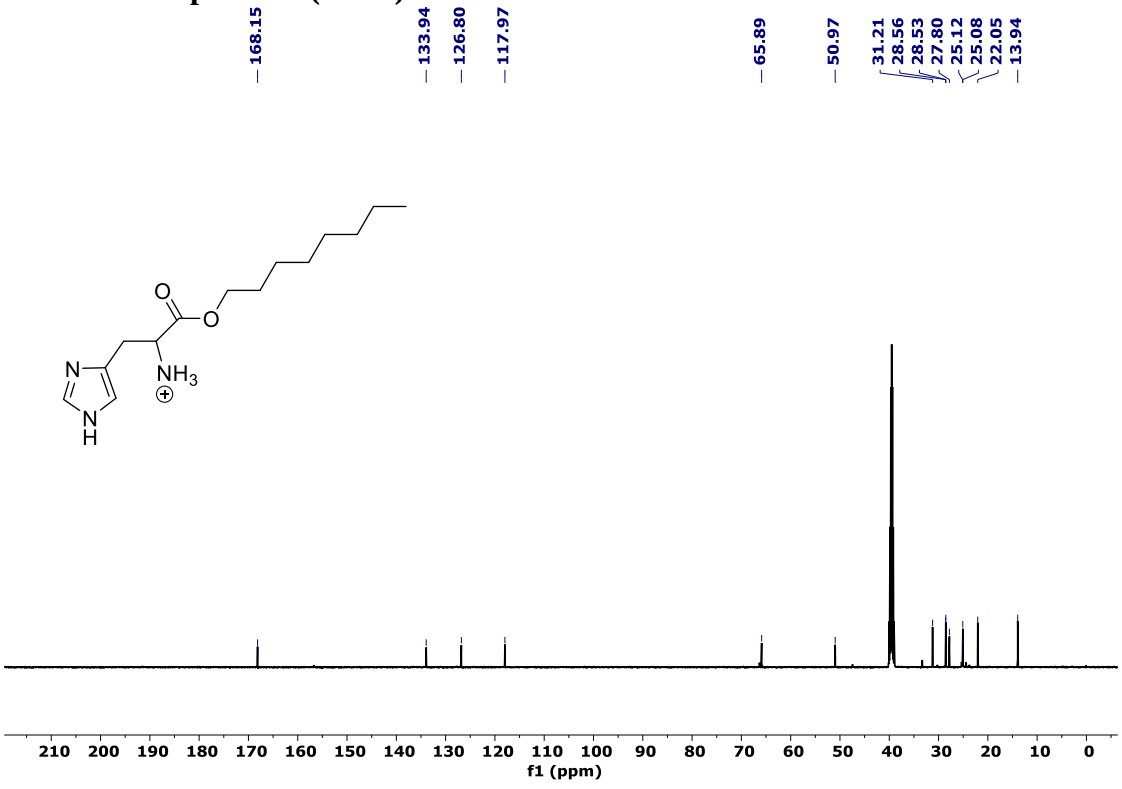

^{1}H-NMR of compound 10 (OBH):

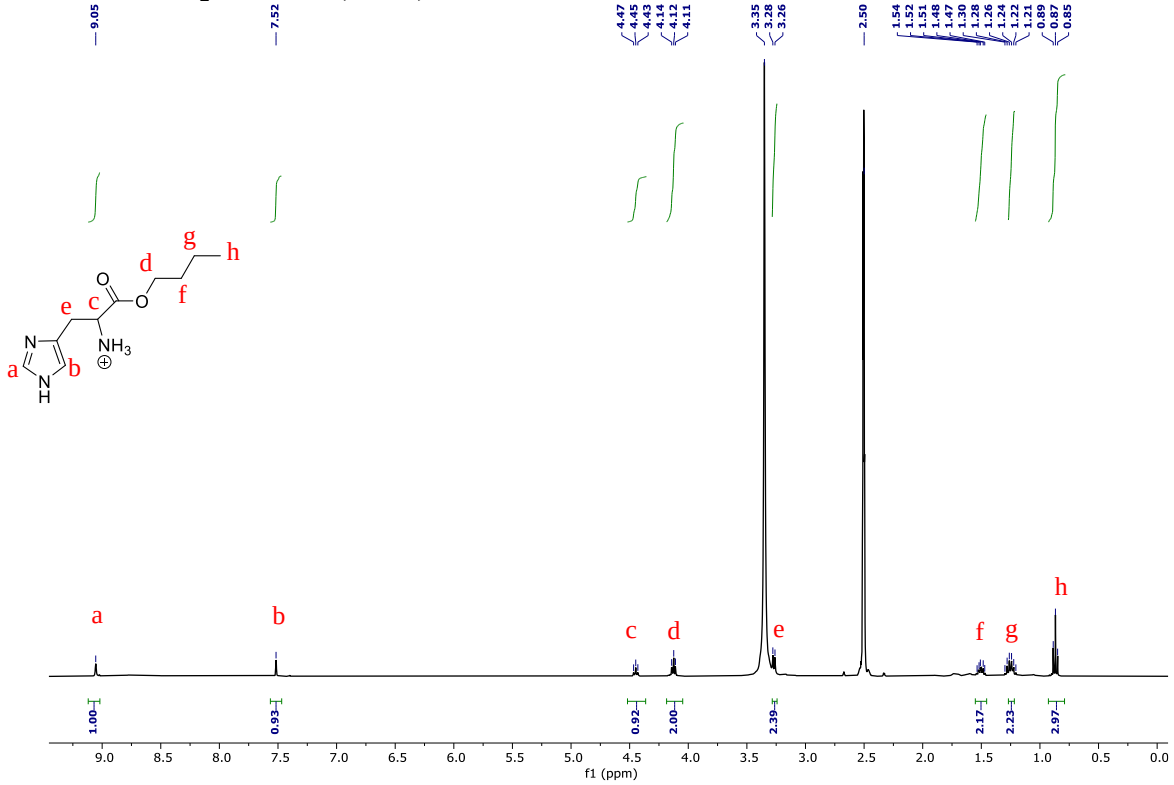

^{13}C-NMR of compound 10 (OBH):

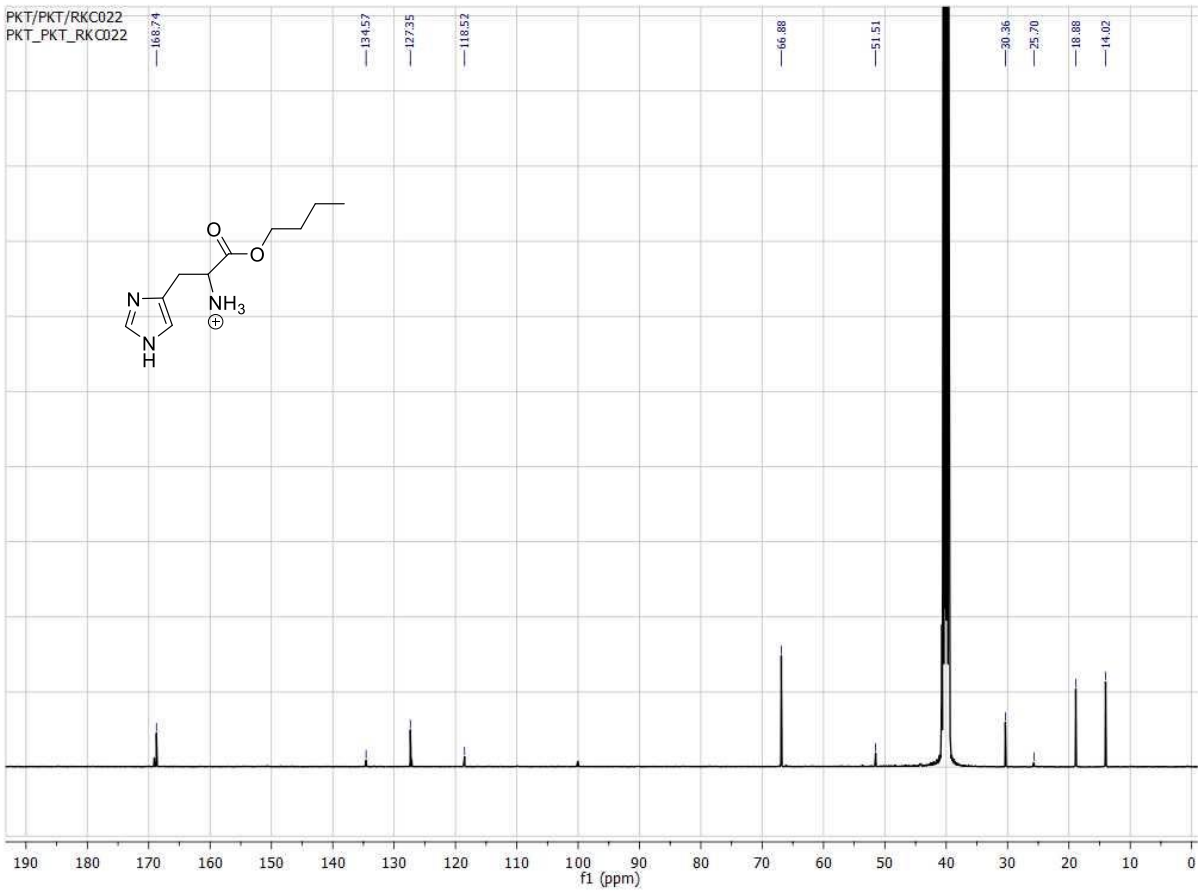

***O*-Lauryl serine (OLS) 14**:

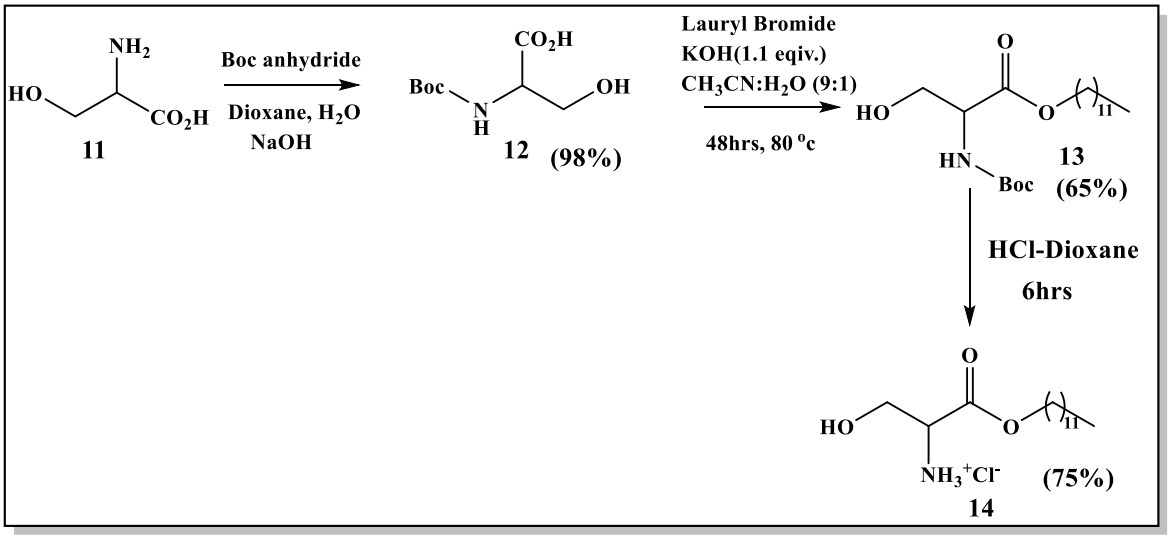

A solution of L-Serine **11** (5 mmol) in a mixture of dioxane (10 ml), water (5 ml) and 1M NaOH (5 ml) was stirred and cooled in an ice bath. Boc anhydride (6 mmol) was added and stirring was continued at room temp. for overnight. Then dioxane was removed from the solution in vacuum. The solution was acidified with a dilute solution of $KHSO_4$ to pH 2-3 in ice-bath. The aqueous phase was extracted with ethyl acetate thrice and solvent was evaporated to get *N*-Boc serine **12**. The yield was found to be 98%.

The esterification of carboxylic acid group was done selectively (in the presence of alcohol group) with lauryl bromide. First, *N*-Boc serine and 1 equivalent of KOH were taken in 18 ml acetonitrile and 2 ml DMF solution (acetonitrile: DMF = 9:1). The solution was stirred for 1 hour at reflux condition at 80 ^oC. After 1 hour, lauryl bromide (1.1 equivalents) was added, and the reaction was allowed to continue for 24 hours at reflux condition. After the reaction was complete, acetonitrile was evaporated under reduced pressure, and the solution was washed with water 5 times to remove extra KOH and DMF. Product **13** was extracted with ethyl acetate and purified by column chromatography. The yield was 65%. Deprotection of the Boc group to get *O*-lauryl serine **14** was carried out using HCl-Dioxane. The yield was 75%. The purity of **14** (OLS) was checked by ^1H NMR (400 MHz, DMSO-D_6) δ 8.50 (s, 3H), 5.60 (t, J = 5.0 Hz, 1H), 4.15 (t, J = 6.5 Hz, 2H), 4.10 (t, J = 3.8 Hz, 1H), 3.82 (d, J = 3.1 Hz, 2H), 1.60 (p, J = 6.5 Hz, 2H), 1.25 (s, 18H), 0.86 (t, J = 6.9 Hz, 3H); ^{13}C NMR (126 MHz, DMSO) δ 168.45, 65.97, 59.98, 54.90, 31.76, 29.52, 29.48, 29.46, 29.40, 29.17, 29.11, 28.45, 25.63, 22.55, 14.38. HRMS [ESI]: $[M+H]^+$ Found: 274.2378, $C_{15}H_{32}NO_3$ requires 274.2382.

^{1}H-NMR of compound 14 (OLS):

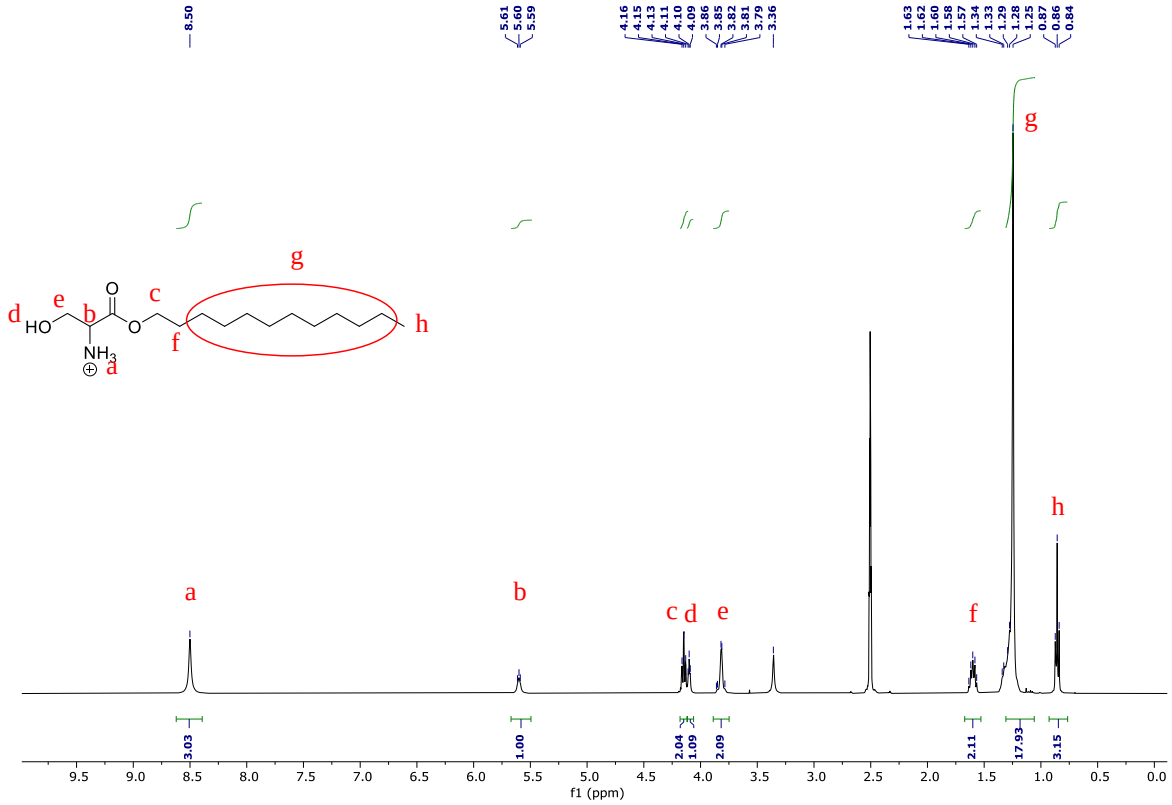

^{13}C-NMR of compound 14 (OLS):

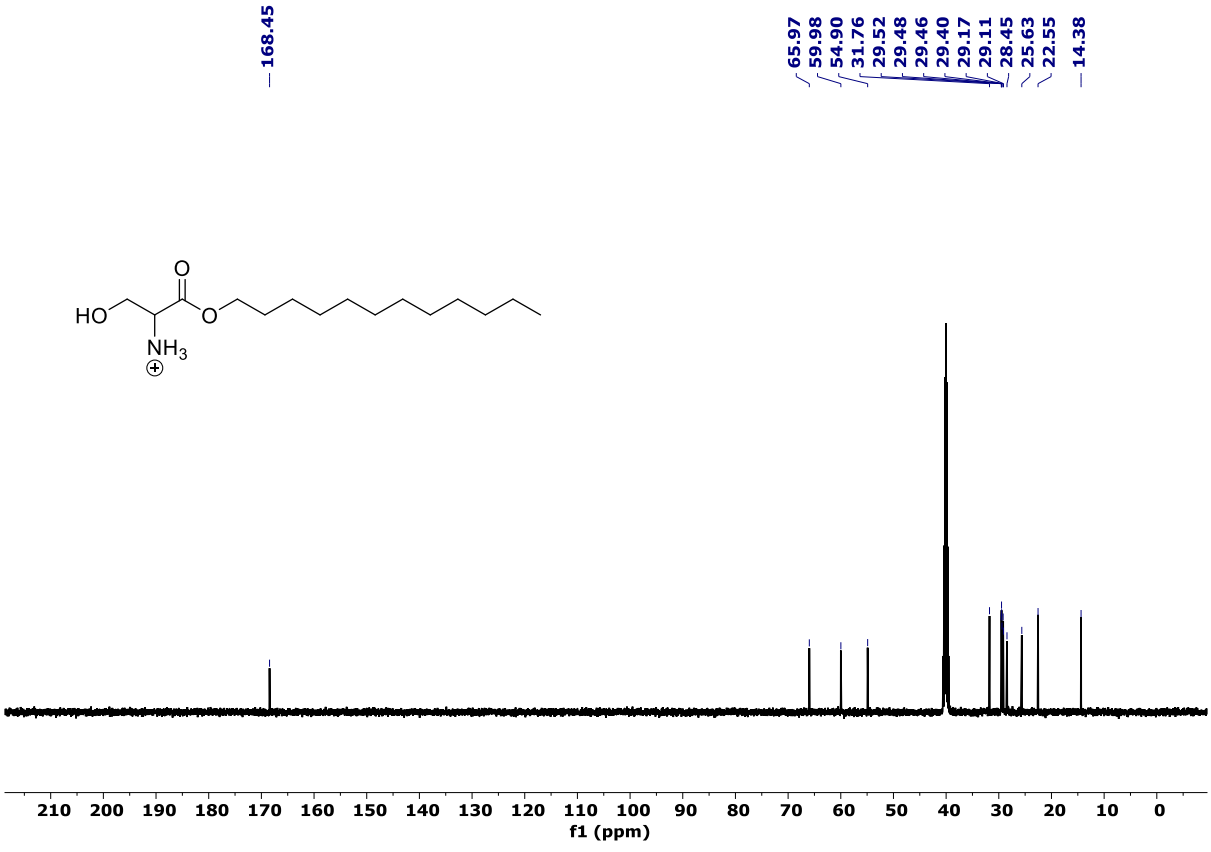

***N*-Lauroyl serine (NLS**) **17**: NLS was synthesized following slight modification of reported procedure.[11, 12]

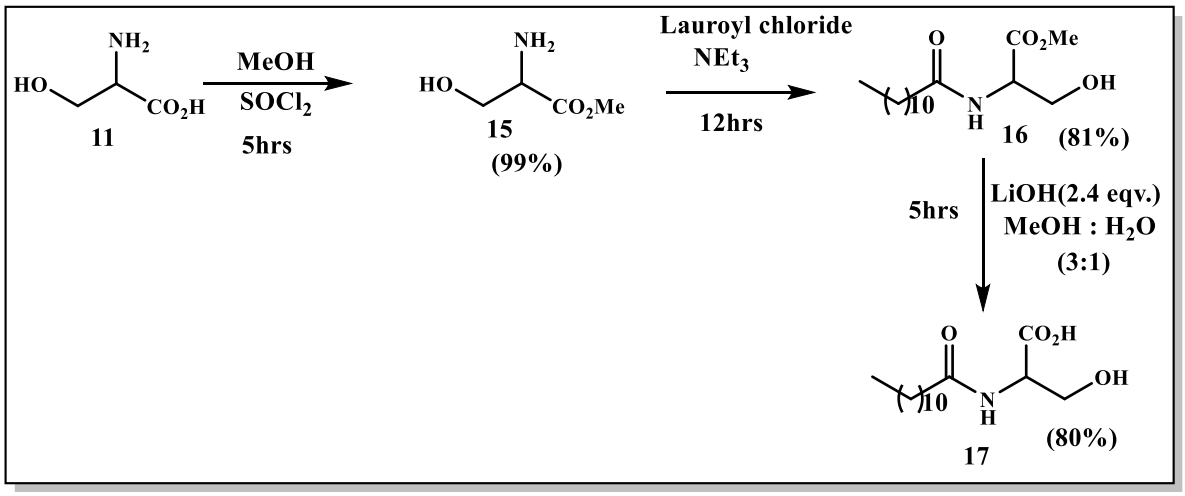

L-Serine **11** was taken in a RB flask, and methanol was added to dissolve it. The RB was kept in ice-cold condition with nitrogen atmosphere and stirred for 10 minutes. Then $SOCl_2$ (4 equivalents) was added to the mixture dropwise. The reaction was allowed to go on for 5 hours. After the reaction was complete the $SOCl_2$ was removed by distillation to get the serine methyl ester **15**. The yield was 99%.

Lauroyl chloride was prepared from lauric acid by using oxalyl chloride (4 equivalents) under nitrogen atmosphere for two hours at room temperature. Then lauroyl chloride was coupled with the amine group of the serine methyl ester to form *N*-lauroyl serine methyl ester **16** in presence of triethyl amine and under an inert atmosphere. Reaction was allowed to go on for 12 hours. The solution was washed with NaOH (2 times), dilute HCl (2 times), and brine (2 times). The yield was 81%.

The methyl groups were deprotected to get *N*-lauroyl serine (NLS) **17**. One equivalent of methyl ester was dissolved in methanol: water (3:1) and kept in ice-cold condition. Approx. 2.4 equivalents of LiOH was added to the ester and stirred for 5 hours. The mixture was acidified at ice-cold condition with HCl. The final compound was extracted with ethyl acetate. The yield was 80%. The purity of NLS (**17)** was checked by NMR spectroscopy, which matches with reported literature.[12] ^{1}H NMR (400 MHz, CHLOROFORM-*D*) δ 6.74 (d, *J* = 7.9 Hz, 1H), 4.40 (dt, *J* = 8.5, 4.3 Hz, 1H), 3.80 (dd, *J* = 11.0, 4.9 Hz, 1H), 3.66 (dd, *J* = 11.3, 4.6 Hz, 1H), 2.43 (s, 1H), 2.09 (q, *J* = 8.2 Hz, 2H), 1.44 (dq, *J* = 13.4, 6.7 Hz, 2H), 1.09 (s, 16H), 0.71 (t, *J* = 6.7 Hz, 3H); HRMS [ESI]: $[M+H]^+$ Found: 288.2164, $C_{15}H_{30}NO_4$ requires 288.2175.

^{1}H-NMR of compound 17 (NLS):

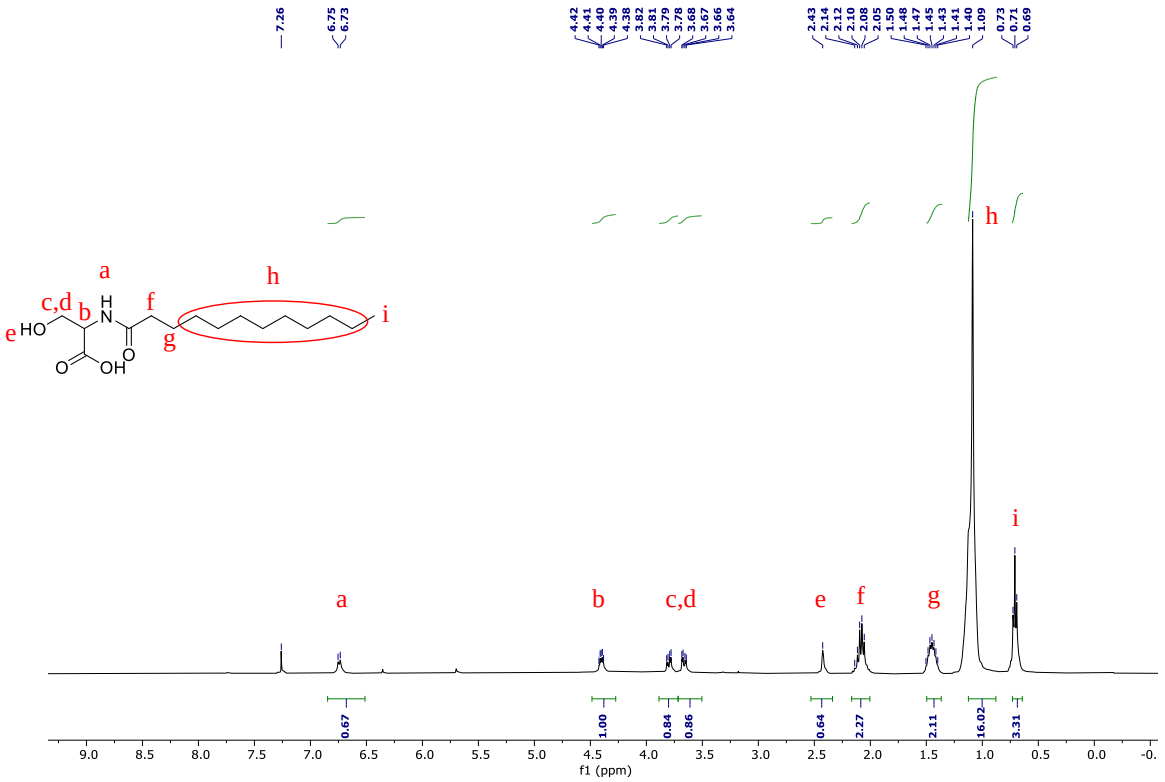

***N*-Lauroyl aspartic acid (NLA) 21:**

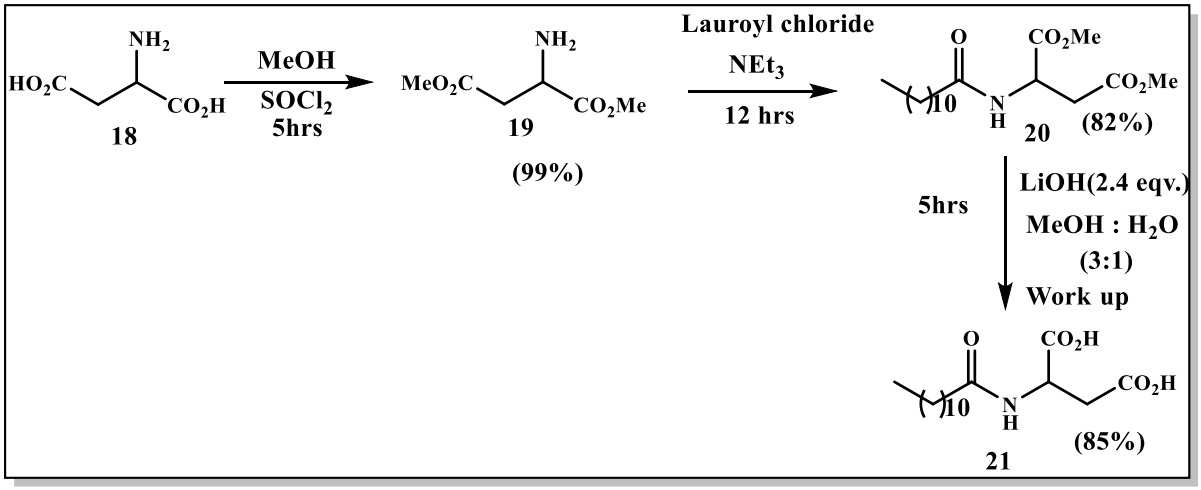

L-Aspartic acid **18** was taken in an RB flask with methanol and was kept in ice-cold condition with nitrogen atmosphere and stirred for 10 minutes. Then $SOCl_2$ (4 equivalents) was added to the mixture dropwise. The reaction was allowed to go on for 5 hours. After the reaction was complete the $SOCl_2$ was removed by distillation to get the aspartic acid methyl ester **19**. The yield was 99%.

Lauroyl chloride was prepared from lauric acid by using oxalyl chloride (4 equivalents) under nitrogen atmosphere for two hours at room temperature. Then lauroyl chloride was coupled with the amine group of the aspartic acid methyl ester to form *N*-lauroyl aspartic acid methyl ester **20** in presence of triethyl amine and under an inert atmosphere. The reaction was allowed to go on for 12 hours. The solution was washed with NaOH (2 times), dilute HCl (2 times), and brine (2 times). The yield was 82%.

The methyl groups were deprotected to get *N*-lauroyl aspartic acid **21**. One eq. of methyl ester was dissolved in methanol: water (3:1) and kept in ice-cold conditions. Approx. 2.4 eq. of LiOH was added to the ester and stirred for 5 hours. The mixture was acidified at ice-cold conditions with HCl up to pH 2.0. The acid was extracted with ethyl acetate. The yield was 85%. The purity of *N*-lauroyl aspartic acid (NLA) **21** was checked by ^{1}H-NMR spectroscopy and Mass spectrometry. ^{1}H NMR (400 MHz, DMSO-D_6) δ 12.47 (s, 2H), 8.09 (d, J = 7.9 Hz, 1H), 4.62 – 4.44 (m, 1H), 2.67 (dd, J = 16.5, 6.1 Hz, 1H), 2.58 – 2.52 (m, 1H), 2.08 (t, J = 7.3 Hz, 2H), 1.46 (p, J = 7.0 Hz, 2H), 1.24 (s, 16H), 0.89 – 0.83 (m, 3H); ^{13}C NMR (126 MHz, DMSO) δ 173.00, 172.55, 172.11, 49.00, 36.56, 35.52, 31.76, 29.50, 29.47, 29.41, 29.27, 29.17, 29.00, 25.66, 22.55, 14.40. HRMS [ESI]: $[M+H]^+$ Found: 316.2115, $C_{20}H_{39}NO_5$ requires 316.2124.

^{1}H-NMR of compound 21 (NLA):

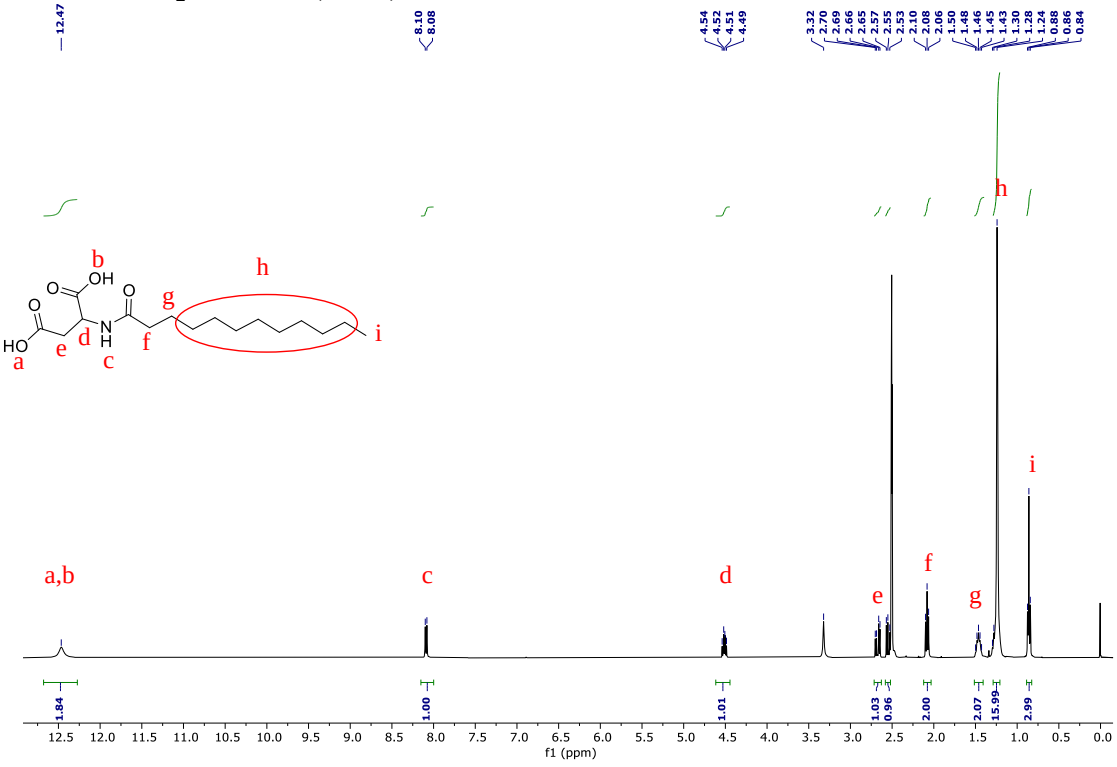

^{13}C-NMR of compound 21 (NLA):

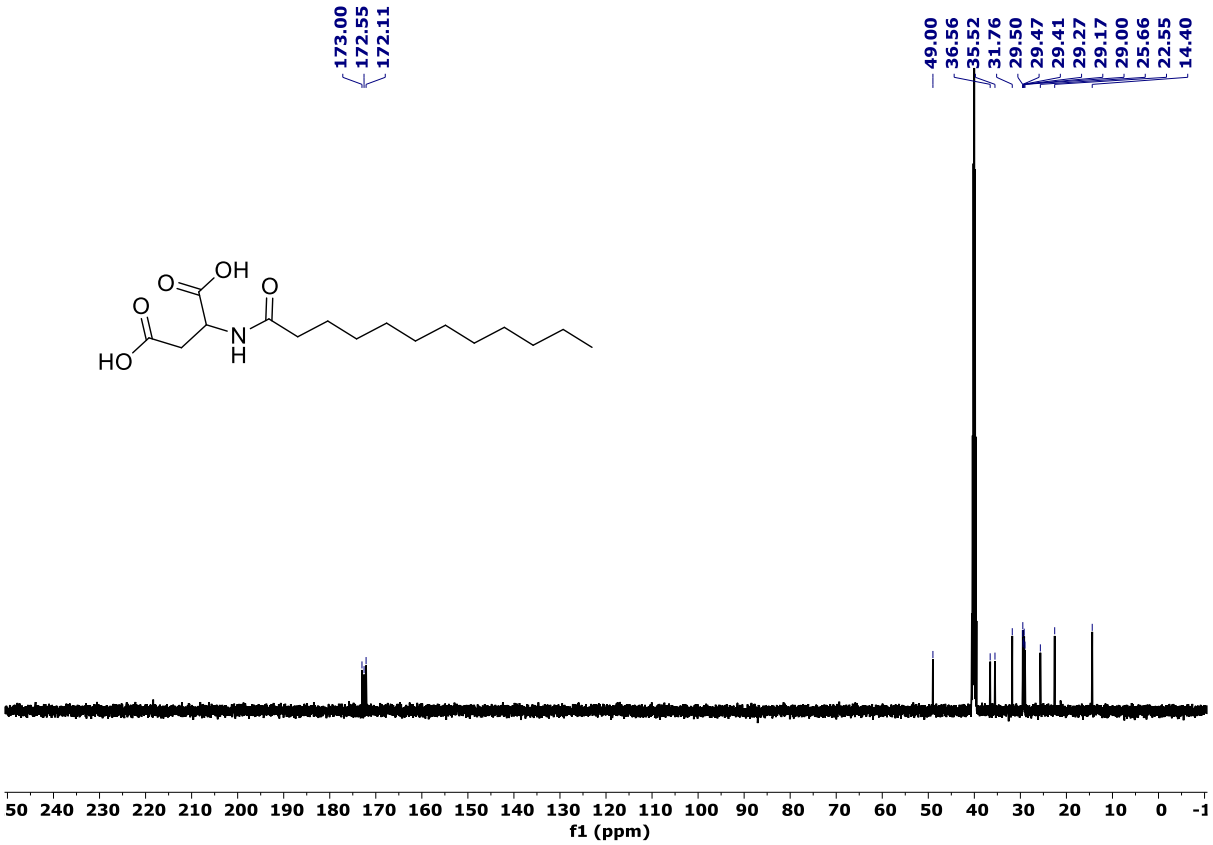

Procedure for substrate(s) synthesis: Compounds (**22-27**) were synthesized following slight modification of the reported procedure.[13, 14] Aliphatic acids (1eqv.) (acetic acid, butyric acid, hexanoic acid, octanoic acid, decanoic acid and lauric acid) was dissolved in dry DCM (10 ml). Then DCC (1.2 eq.), DMAP (0.2 eq.) and *p*-nitro phenol (1.0 eq.) was added to the reaction mixture, and the reaction mixture was stirred for 24 hrs at room temperature. After completion of the reaction, the reaction mixture was concentrated under reduced pressure and dissolved in ethyl acetate and filtered to remove DCU. The filtrate was concentrated under reduced pressure, and the residue was purified by flash chromatography (EtOAc/Hexane 1:20) to give pure compound **22** (82%, white solid),[13] **23** (84%, pale-yellowish liquid),[13] **24** (85%, pale-yellowish liquid),[13, 15] **25**(87%, pale-yellowish liquid),[14] **26** (82%, white solid),[13, 15] **27** (90%, white solid).[13, 16]

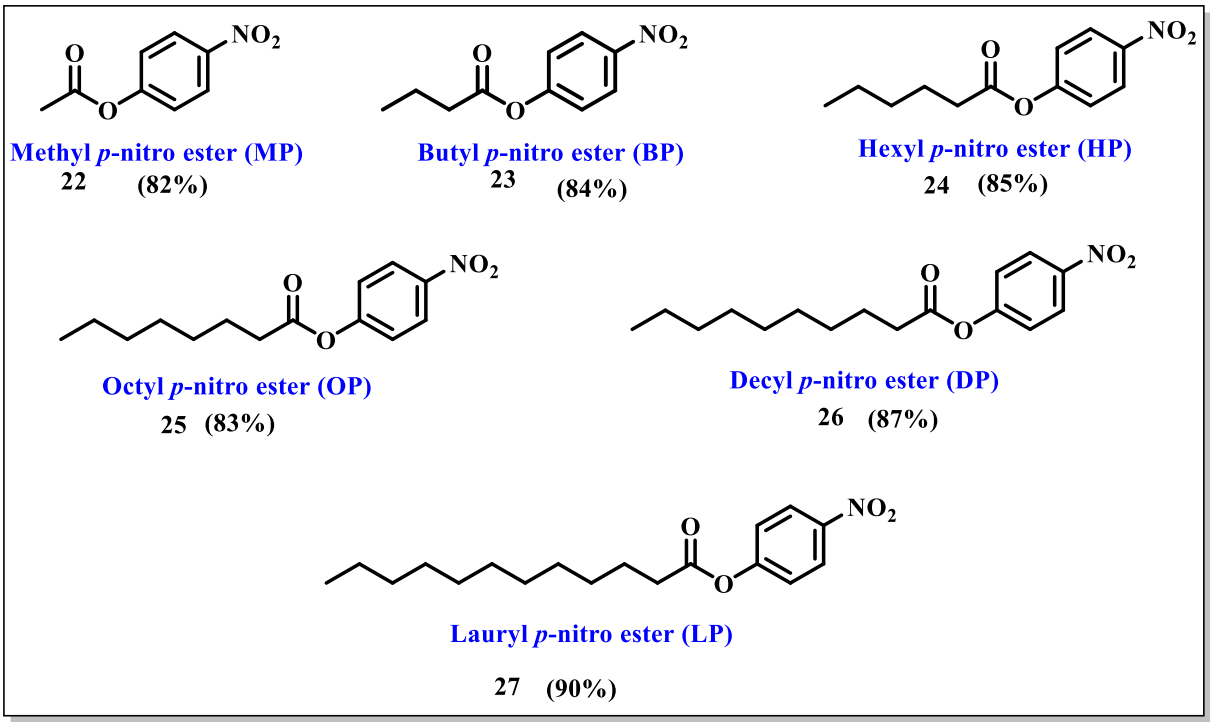

Compound 22 (MP): The purity of the compound (**22)** was checked by NMR spectroscopy, which matches well with reported literature.[13]

^{1}H NMR (400 MHz, CHLOROFORM-*D*) δ 8.27 (d, *J* = 9.1 Hz, 2H), 7.28 (d, *J* = 9.1 Hz, 2H), 2.35 (s, 3H).

Compound 23 (BP): The purity of the compound (**23)** was checked by NMR spectroscopy, which matches well with reported literature.[14]

^{1}H NMR (400 MHz, CHLOROFORM-*D*) δ 8.25 (d, *J* = 9.0 Hz, 2H), 7.25 (d, *J* = 9.0 Hz, 2H), 2.57 (t, *J* = 7.5 Hz, 2H), 1.78 (h, *J* = 7.5 Hz, 2H), 1.03 (t, *J* = 7.3 Hz, 3H).

Compound 24 (HP): The purity of the compound (**24)** was checked by NMR spectroscopy, which matches well with reported literature.[15]

^{1}H NMR (400 MHz, CHLOROFORM-*D*) δ 8.25 (d, *J* = 9.0 Hz, 2H), 7.26 (d, *J* = 9.4 Hz, 2H), 2.58 (t, *J* = 7.4 Hz, 2H), 1.75 (p, *J* = 7.4 Hz, 2H), 1.43 – 1.29 (m, 4H), 0.92 (t, *J* = 8.0 Hz, 3H).

Compound 25 (OP): The purity of the compound (**25)** was checked by NMR spectroscopy, which matches well with reported literature.[14]

^{1}H NMR (400 MHz, CHLOROFORM-*D*) δ 8.25 (d, *J* = 9.1 Hz, 2H), 7.25 (d, *J* = 9.1 Hz, 2H), 2.58 (t, *J* = 7.6 Hz, 2H), 1.74 (p, *J* = 7.5 Hz, 2H), 1.38 – 1.25 (m, 8H), 0.87 (t, *J* = 8.0 Hz, 3H).

Compound 26 (DP): The purity of the compound (**26)** was checked by NMR spectroscopy, which matches well with reported literature.[15]

^{1}H NMR (400 MHz, CHLOROFORM-*D*) δ 8.25 (d, *J* = 9.1 Hz, 2H), 7.25 (d, *J* = 9.0 Hz, 2H), 2.58 (t, *J* = 7.4 Hz, 2H), 1.74 (p, *J* = 7.4 Hz, 2H), 1.40 – 1.23 (m, 12H), 0.87 (t, *J* = 8.0 Hz, 3H).

Compound 27 (LP): The purity of the compound (**27)** was checked by NMR spectroscopy, which matches well with reported literature.[16]

^{1}H NMR (400 MHz, CHLOROFORM-*D*) δ 8.25 (d, *J* = 9.0 Hz, 2H), 7.26 (d, *J* = 9.0 Hz, 2H), 2.58 (t, *J* = 7.4 Hz, 2H), 1.74 (p, *J* = 7.5 Hz, 2H), 1.41 – 1.17 (m, 16H), 0.86 (t, *J* = 6.8 Hz, 3H).

^{1}H-NMR of compound 22 (MP):

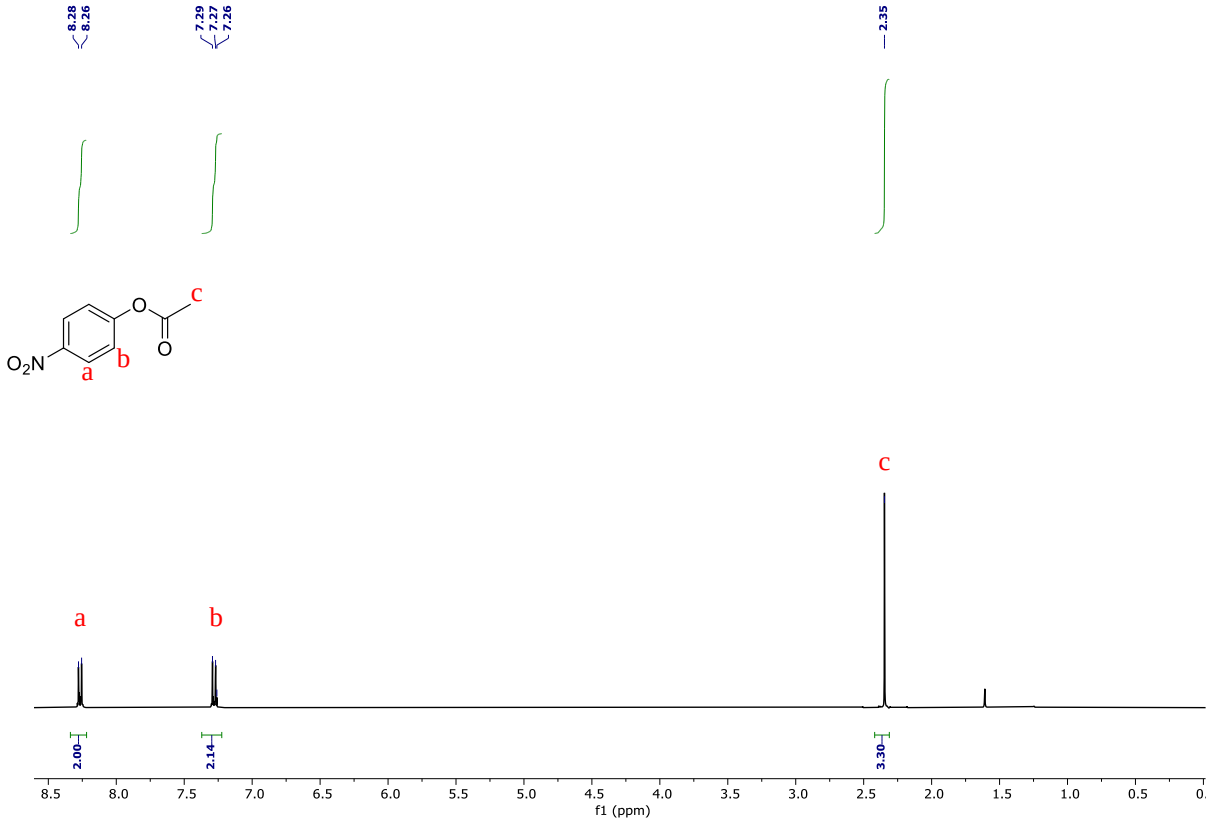

^{1}H-NMR of compound 23 (BP):

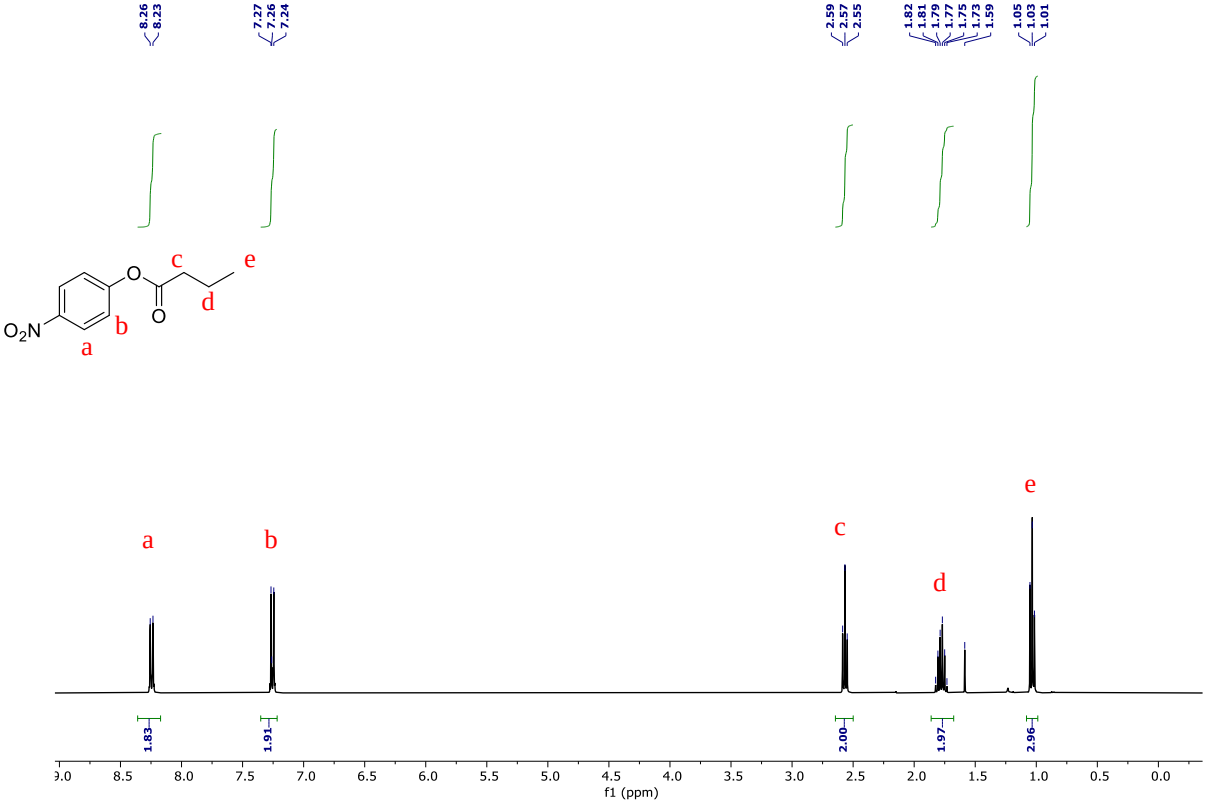

^{1}H-NMR of compound 24 (HP):

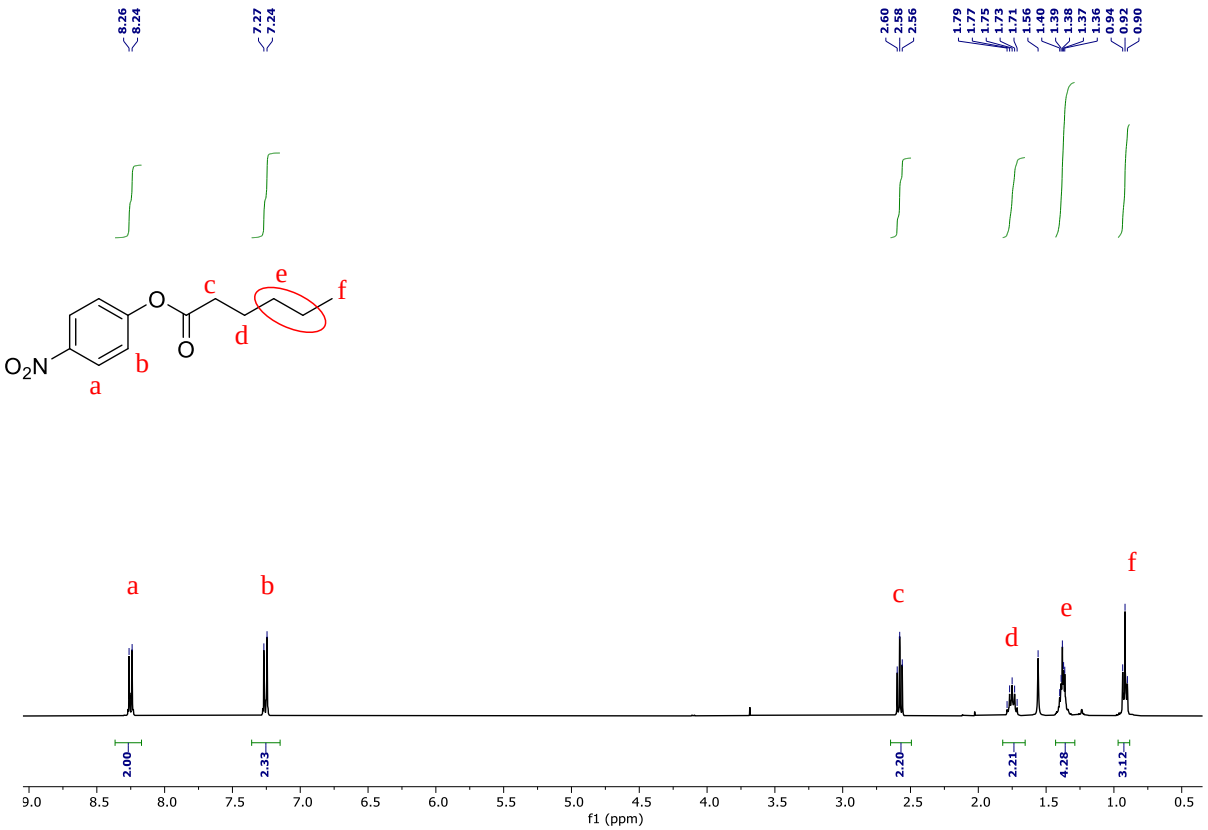

^{1}H-NMR of compound 25 (OP):

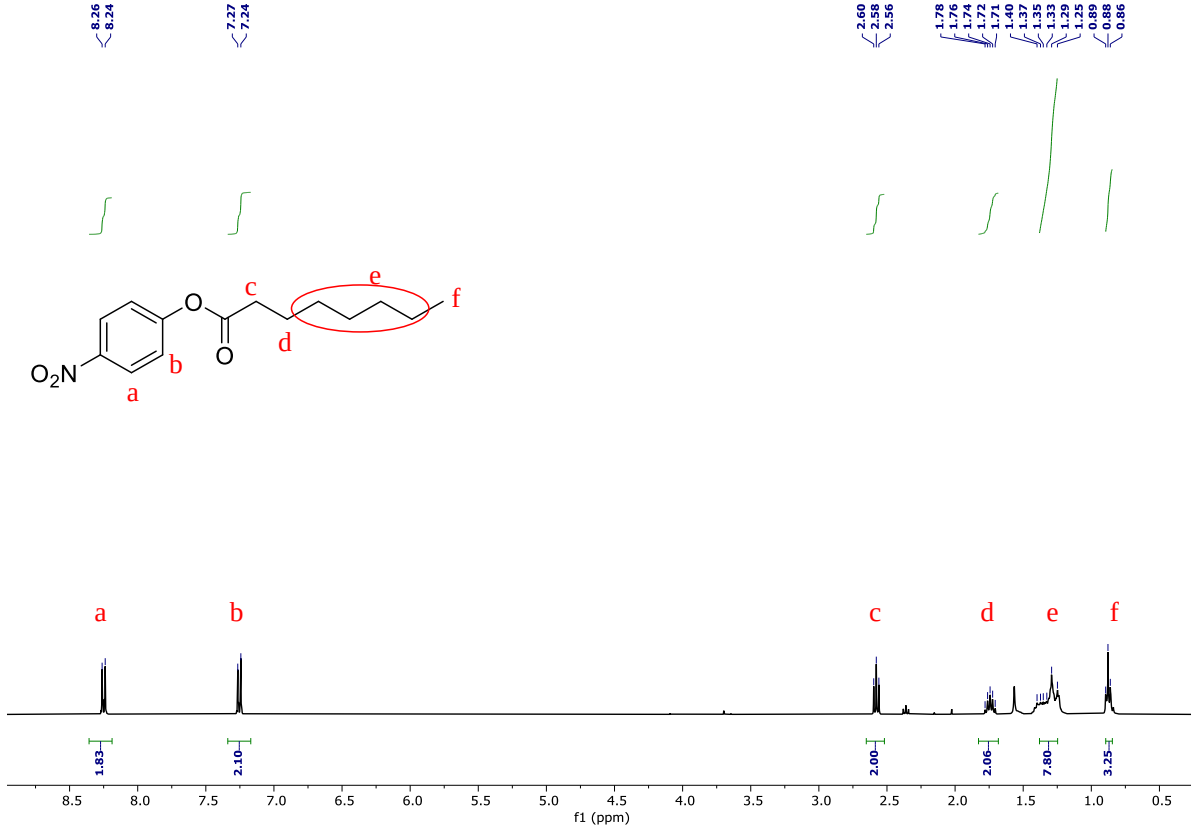

^{1}H-NMR of compound 26 (DP):

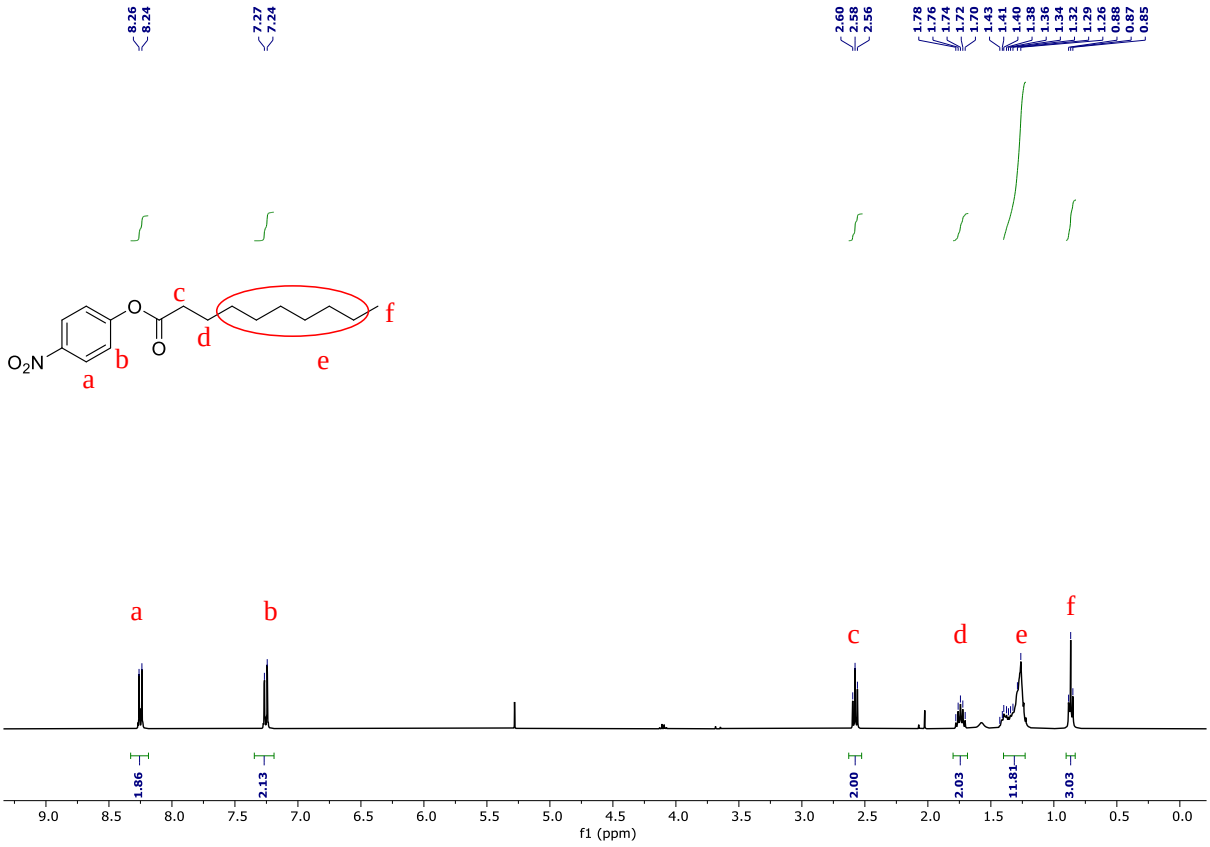

^{1}H-NMR of compound 27 (LP):

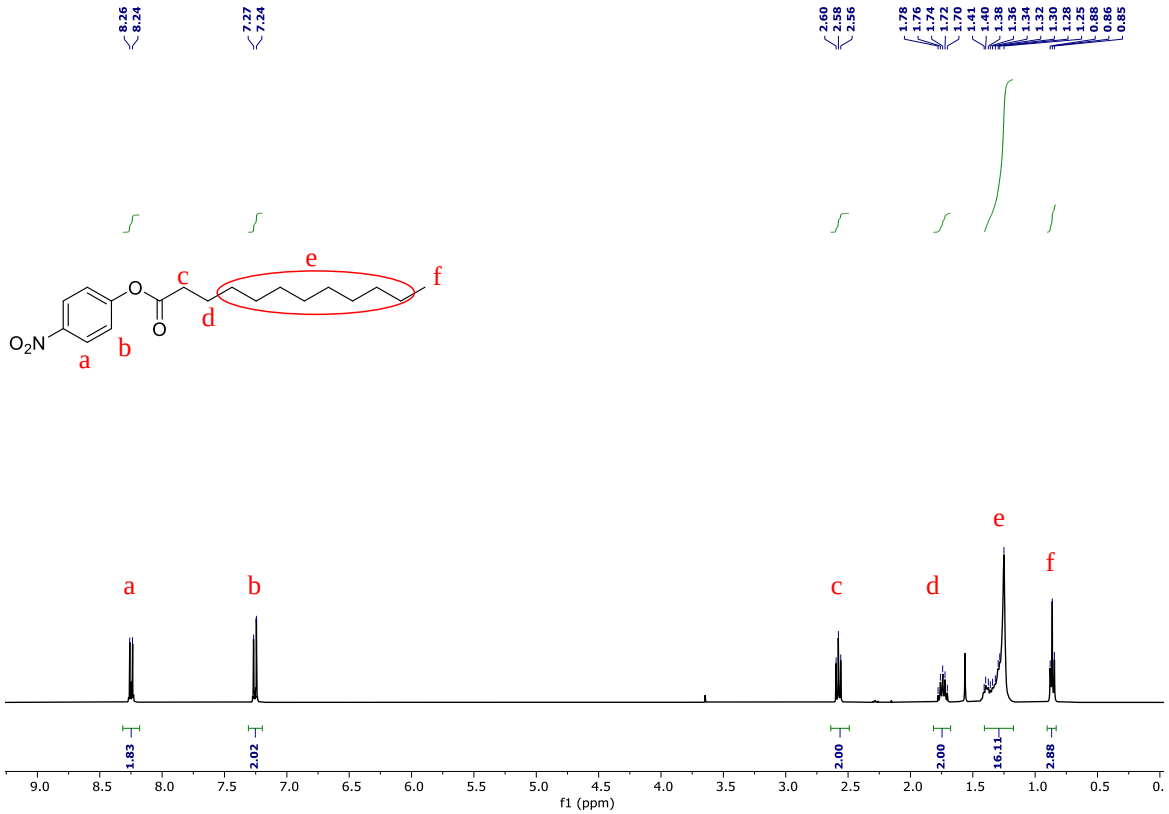

References

1. O. A. El Seoud, *Advances in Colloid and Interface Science*, 1989, **30**, 1-30.
2. M. D. Nothling, A. Ganesan, K. Condic-Jurkic, E. Pressly, A. Davalos, M. R. Gotrik, Z. Xiao, E. Khoshdel, C. J. Hawker, M. L. O'Mara, M. L. Coote and L. A. Connal, *Chem*, 2017, **2**, 732-745.
3. A. Kumar, M. D. Nothling, H. M. Aitken, Z. Xiao, M. Lam, C. A. Bell, M. L. O'Mara and L. A. Connal, *Catalysis Science & Technology*, 2022, **12**, 6655-6659.
4. M. D. Nothling, Z. Xiao, N. S. Hill, M. T. Blyth, A. Bhaskaran, M.-A. Sani, A. Espinosa-Gomez, K. Ngov, J. White, T. Buscher, F. Separovic, M. L. O'Mara, M. L. Coote and L. A. Connal, *Science Advances*, 2020, **6**, eaaz0404.
5. C. Zhang, X. Xue, Q. Luo, Y. Li, K. Yang, X. Zhuang, Y. Jiang, J. Zhang, J. Liu, G. Zou and X.-J. Liang, *ACS Nano*, 2014, **8**, 11715-11723.
6. K. Gayen, K. Basu, D. Bairagi, V. Castelletto, I. W. Hamley and A. Banerjee, *ACS Applied Bio Materials*, 2018, **1**, 1717-1724.
7. P. Dowari, M. Kumar Baroi, T. Das, B. Kanti Das, S. Das, S. Chowdhuri, A. Garg, A. Debnath and D. Das, *Journal of Colloid and Interface Science*, 2022, **618**, 98-110.
8. N. Singh, M. P. Conte, R. V. Ulijn, J. F. Miravet and B. Escuder, *Chemical Communications*, 2015, **51**, 13213-13216.
9. M. O. Guler and S. I. Stupp, *Journal of the American Chemical Society*, 2007, **129**, 12082-12083.
10. Z. Wang, Y. Lu, J. Yang, W. Xiao, T. Chen, C. Yi and Z. Xu, *Langmuir*, 2023, DOI: 10.1021/acs.langmuir.3c00486.
11. W. H. Qiao and Y. Y. Qiao, *J Surfactants Deterg*, 2013, **16**, 821-828.
12. C. W. Phoon, B. Somanadhan, S. C. H. Heng, A. Ngo, S. B. Ng, M. S. Butler, A. D. Buss and M. M. Sim, *Tetrahedron*, 2004, **60**, 11619-11628.

13. L. Qian, J.-Y. Liu, J.-Y. Liu, H.-L. Yu, C.-X. Li and J.-H. Xu, *Journal of Molecular Catalysis B: Enzymatic*, 2011, **73**, 22-26.
14. M. D. Arifuzzaman and Y. Zhao, *ACS Catalysis*, 2018, **8**, 8154-8161.
15. C. J. Hastings, M. S. DiNola, E. Petratos and E. J. Veltri, *Tetrahedron*, 2023, **133**, 133271.
16. S. V. A. M. Legendre, M. Jevric, J. Klepp, C. J. Sumby and B. W. Greatrex, *Tetrahedron*, 2018, **74**, 1229-1239.